AD_____

Award Number: W81XWH-05-1-0065

TITLE: Inhibition of Fatty Acid Synthase in Prostate Cancer by Olristat, a Novel Therapeutic

PRINCIPAL INVESTIGATOR: Steven J. Kridel, Ph.D.

CONTRACTING ORGANIZATION: Wake Forest University Health Sciences
Winston-Salem, NC 27157

REPORT DATE: November 2006

TYPE OF REPORT: Annual

PREPARED FOR: U.S. Army Medical Research and Materiel Command
Fort Detrick, Maryland 21702-5012

REPORT DOCUMENTATION PAGE

Form Approved
OMB No. 0704-0188

1. REPORT DATE	2. REPORT TYPE	3. DATES COVERED
01-11-2006	Annual	1 Nov 2005 – 31 Oct 2006

4. TITLE AND SUBTITLE

Inhibition of Fatty Acid Synthase in Prostate Cancer by Olristat, a Novel Therapeutic

5a. CONTRACT NUMBER

5b. GRANT NUMBER
W81XWH-05-1-0065

5c. PROGRAM ELEMENT NUMBER

6. AUTHOR(S)

Steven J. Kridel, Ph.D.

Email: skridel@wfubmc.edu

5d. PROJECT NUMBER

5e. TASK NUMBER

5f. WORK UNIT NUMBER

7. PERFORMING ORGANIZATION NAME(S) AND ADDRESS(ES)

Wake Forest University Health Sciences
Winston-Salem, NC 27157

8. PERFORMING ORGANIZATION REPORT NUMBER

9. SPONSORING / MONITORING AGENCY NAME(S) AND ADDRESS(ES)
U.S. Army Medical Research and Materiel Command
Fort Detrick, Maryland 21702-5012

10. SPONSOR/MONITOR'S ACRONYM(S)

11. SPONSOR/MONITOR'S REPORT NUMBER(S)

12. DISTRIBUTION / AVAILABILITY STATEMENT
Approved for Public Release; Distribution Unlimited

13. SUPPLEMENTARY NOTES
Original contains colored plates: ALL DTIC reproductions will be in black and white.

14. ABSTRACT The overall goal of this project s to understand the anti-tumor effects of FAS inhibitors. We have followed up on our previous findings by further evaluating the role of ER stress in tumor cells treated with FAS inhibitors. Our results suggest that ER stress may initiate the cell death program when FAS is inhibited in prostate tumor cell lines. Moreover, the data also suggest that the ER may sense fatty acid levels in tumor cells. A further connection to ER stress was discovered by showing that other ER stressing agents like Velcade induce fatty acid synthase activity and sensitize cells to the effects of FAS inhibitors. We have also made the novel observation that FAS expression is regulated by the src oncogene and that FAS inhibitors can block src driven matrigel invasion. Combined these data provide insight into how disruption of the FAS axis can be further exploited to inhibit prostate tumor growth and metastases. We have also extended our previous crystallography studies by solving the crystal structure of FAS bound to a cleaved orlistat. These data will provide valuable insight into future drug discovery and design within the FAS pathway. In total, we have made great strides toward understanding the anti-tumor effects of orlistat and other FAS inhibitors in prostate cancer through a multi-disciplinary approach combining cell biology, biochemistry and crystallography.

15. SUBJECT TERMS
Fatty acid synthase, orlistat, inhibitor, endoplasmic reticulum stress, apoptosis, crystallography, prostate cancer

16. SECURITY CLASSIFICATION OF:			17. LIMITATION OF ABSTRACT	18. NUMBER OF PAGES	19a. NAME OF RESPONSIBLE PERSON
a. REPORT	b. ABSTRACT	c. THIS PAGE			USAMRMC
U	U	U	UU	56	19b. TELEPHONE NUMBER *(include area code)*

Table of Contents

A. Introduction

This is the annual report for grant # W81XWH-05-1-0065 entitled "Inhibition of Fatty Acid Synthase by Orlistat: A Novel Therapeutic". The funding period for this grant began on November 1, 2004. In the period since the funding date, significant progress has been made. Since the last report, we have presented two abstracts at national meetings and have had one paper published and another accepted for publication. The details of our recent findings are discussed in full in section C. The three specific aims of the grant are listed below.

Specific Aim 1. *To determine the cellular consequences of FAS inhibition by orlistat.* The purpose of this aim is to determine the mechanism behind the anti-tumor effect of orlistat by examining activation of various apoptotic pathways in orlistat treated cells.
Specific Aim 2. *To analyze the molecular basis of FAS inhibition by orlistat.* The goal of this aim is to determine the structure of the thioesterase domain of FAS bound to a novel inhibitor orlistat. We hypothesize that by determining this structure was can design orlistat-like compounds that have better inhibitor specificity and bioavailability.
Specific Aim 3. *To select and characterize novel FAS inhibitor scaffolds using peptide phage display.* The purpose of this aim is to use phage display to derive novel chemical scaffolds that can be used to design optimized FAS inhibitors.

B. Body

FAS Activity and the Endoplasmic Reticulum Stress Response. It has been hypothesized that a primary role for FAS in tumor cells is membrane biogenesis (1). In support of this premise, Swinnen et al. demonstrated that the product of FAS activity, the 16-carbon fatty acid palmitate segregates to detergent- insoluble, membrane domains (2). Phosphatidylcholine (PC) is the phospholipid that palmitate preferentially segregates into. PC is also the primary phospholipid of the endoplasmic reticulum (ER). Interestingly, inhibition of the rate-limiting step of PC biosynthesis, CTP:phosphocholine cytidylyltransferase (CT), by chemical inhibitors or by expression of a temperature sensitive mutant, activates the ER stress response to induce apoptosis (3). Because of the connections between FAS activity and membrane biogenesis, we tested the hypothesis that FAS inhibition activates the ER stress response. As described in the subsequent section, we have demonstrated that FAS inhibition does activate the ER stress response, likely due to depleted palmitate for membrane biogenesis. We have also shown that the ER stress response is a primary activator of apoptosis following FAS inhibition, and that FAS inhibition can synergize with another ER stressor, thapsigargin (Tgn).

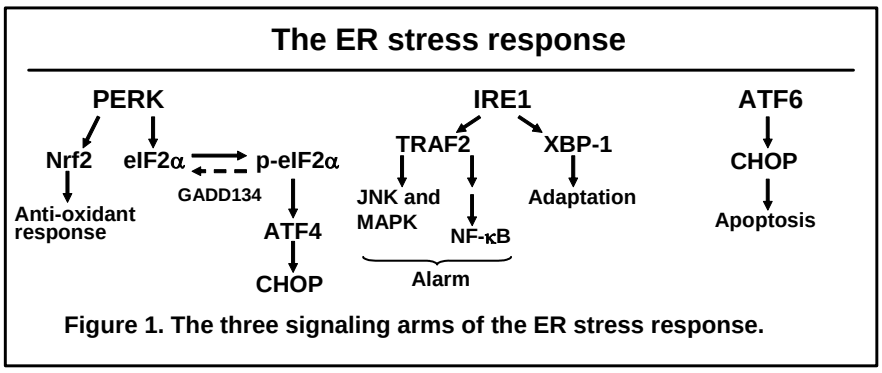

Figure 1. The three signaling arms of the ER stress response.

The ER stress response (Fig.1) is activated by an accumulation of unfolded proteins in the ER as part of the unfolded protein response (UPR) (4-7). The ER stress response is causally associated with diabetes, neurodegenerative disorders, and other maladies (4-7). In addition, ER stress is also associated with tumor growth (5, 8). Typically, proteins destined for secretion are translated into the ER. Chaperones and other foldases promote proper protein folding and secretion. If proper folding is not accomplished, proteins are degraded and shuttled out of the ER in a process termed ER-associated degradation (ERAD) (38). However, under chronic stress, unfolded proteins accumulate and activate the ER stress response. ER stress is characterized by activation of three signaling arms; PERK, IRE1 and ATF6 (7, 9). In the first signaling arm of the ER stress response, the double-stranded RNA-activated

protein kinase (PKR)-like endoplasmic reticulum kinase (PERK) phosphorylates the translation initiation factor eIF2α (10, 11). Phosphorylation of eIF2α activates the expression of the transcription factor ATF4 and the subsequent activation of downstream targets via alternate upstream ORF's (11). The transcription factor Nrf2, part of the Nrf2-Keap1 complex that regulates the response to redox imbalance, has also been identified as a target of PERK activity (12, 13). Our preliminary data suggests that Nrf2 may be activated when FAS is inhibited. Activation of the inositol requiring kinase 1 (IRE1) is the second arm of the ER stress response (14). The IRE1 kinase also encodes an endoribonuclease activity that, when activated, results in splicing of the X-box binding protein-1 (XBP-1) transcription factor mRNA, resulting in a short form of XBP-1 (XBP-1s) (15, 16). XBP-1s is a transcription factor that is primarily responsible for transcription of genes that participate in increasing ER volume during ER stress to accommodate accumulated proteins (17, 18). The IRE1 pathway also activates the JNK, MAPK and NF-κB signaling pathways (9, 19, 20). The latter two are also activated when FAS activity is inhibited (21). The third arm of the ER stress response is the activation of the transcription factor ATF6. After proteolytic activation in the golgi, ATF6 activates the expression of other transcription factors, such as the CCAAT/enhance-binding protein (C/EBP) homologous protein (CHOP) that is implicated in apoptosis (22). Together, the three pathways outlined above regulate the cellular response to ER stress. Several reports have demonstrated the overexpression of ER stress associated proteins in human tumors, tumor cell lines and animal models of cancer, indicating that the response is activated in tumors (5, 8, 23-25).

C.

Aim 1: To determine the cellular consequences of FAS inhibition by orlistat

We have recently demonstrated that FAS inhibitors induce endoplasmic reticulum (ER) stress in tumor cells but not in normal fibroblasts. This data was first reported in the previous summary and a manuscript that was recently accepted for publication in *Cancer Research* is included for reference. The data will not be discussed here as a result. In summary, the data provide the first evidence that FAS inhibitors induce cell death via the ER and provides important insight regarding the anti-tumor effects of FAS inhibitors. The data also provide the first evidence that FAS is important for regulating ER homeostasis in tumor cells and suggests that the ER may act as a sensor of fatty acid levels.

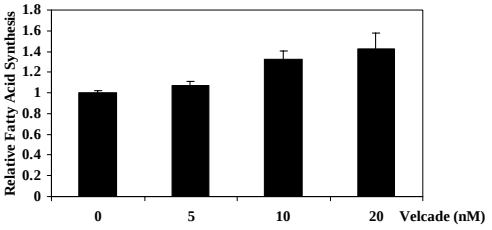

Figure 2. Velcade induces FAS activity. PC-3 cells in 24-well plates were incubated with 14C-acetate for 3 hours. Cell were collected, lysed and extracted. The extracted material was subjected to scintillation counting to quantify fatty acid synthesis.

A body of literature has provided a strong link between ER function and phospholipid and sterol metabolism (3, 18, 26-28). Based on our recent findings that FAS is important for ER function and that FAS inhibitors induce ER stress, we investigated the link between ER stress and FAS activity. The FDA approved proteasome inhibitor Velcade is a known ER stressing agent by inhibiting ER associated protein degradation (29, 30). As a corollary to our findings, Velcade induces a dose-dependent increase in FAS activity in prostate tumor cells (Figure 2). FAS protein levels are not affected by Velcade treatment however (not shown). Interestingly, another ER stressing agent, tunicamycin, also increases FAS activity (data not shown). Thus, it appears that fatty acid synthesis is required as part of the program to respond to ER stress. Because of this, we reasoned that orlistat, through its ability to inhibit FAS, could synergize with Velcade to kill prostate tumor cells. In fact, orlistat and C75, another FAS inhibitor, both synergize with Velcade to inhibit clonogenic survival of prostate tumor cells. In addition, the combination of orlistat, or C75, with Velcade increased levels of cleaved PARP and cleaved

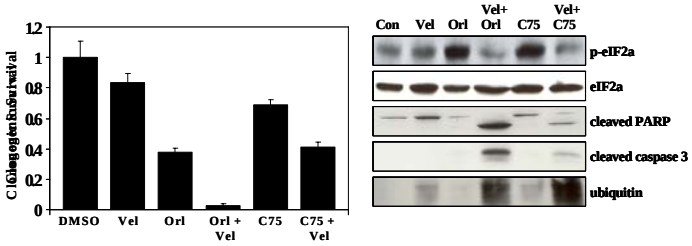

Figure 3. Velcade sensitized cells to FAS inhibition. PC-3 cells were treated with vehicle, Velcade, orlistat or orlistat + Velcade or C75 and C75+Velcade. Clonogenic survival (left) was measured (left) as was markers of ER stress and apoptosis by western blot (right).

caspase-3 compared to either agent alone. Combined, these data demonstrate two important points: 1) that fatty acid synthesis is important in maintaining ER homeostasis and as part of the ER stress response and 2) that FAS inhibitors might be combined with other ER stressing agents like Velcade to more effectively inhibit prostate tumor growth. In total, these data provide valuable insight regarding the anti-tumor effects of orlistat, specifically, and FAS inhibitors in general, and of the biological role of FAS in tumors.

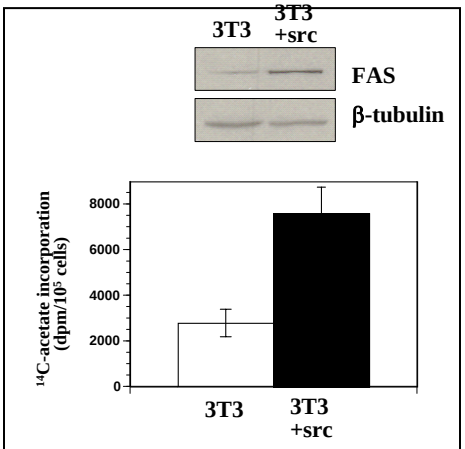

Figure 4. c-src upregulates FAS. Mouse 3T3 cells were transformed with src. FAS expression was determined by immunoblot (top) following src transformation. FAS activity was measured by 14C-acetate icorporation in 3T3 and src transformed 3T3 cells (bottom).

In order to understand how FAS inhibitors could be more effectively used to treat prostate cancer, it is important to understand how FAS expression is regulated in tumors. Previous reports have demonstrated that PI3-kinase, Her2/neu and the androgen receptor are important positive regulators of FAS expression and activity(31-33). We recently identified the oncogene c-src as a novel regulator of FAS expression. Expression of a constitutively active src is sufficient to increase FAS expression and activity roughly 3-fold in mouse 3T3 cells (Figure 4). Previous reports have also demonstrated that expression of constitutively active c-src is sufficient to induce an invasive phenotype (34). Because of the newly discovered connection between src and FAS activity we asked whether FAS inhibitors could inhibit src driven invasion. Interestingly, the FAS inhibitor C75 and TOFA, an inhibitor acetyl coA carboxylase (ACC), the enzyme upstream of FAS, are both effective at completely blocking src driven invasion of 3T3 cells through matrigel (data not shown). This experiment has only been performed twice in triplicate and is not included because of the preliminary nature of the data. However, the data is the first to demonstrate that in addition to inhibiting to growth of primary tumors, FAS inhibitors can potentially inhibit invasion. Because invasion is often used to gauge metastatic potential, these data suggest that inhibition of the FAS pathway could also prevent metastasis, the leading cause of death among men with prostate cancer. In support of this hypothesis, a previous study demonstrated that FAS levels correlate with metastatic potential in prostate cancer (35). There is no literature that describes a role for endogenous fatty acid metabolism on prostate tumor cell motility or invasion. We will follow up on these preliminary studies by determining the effects of src specific inhibitors on FAS activity and expression in prostate tumor cell lines and how FAS inhibitors effect motility and invasion of prostate cancer cell lines.

In addition to the work outlined above and included in the attached manuscript, our work initiated a collaboration that resulted in the first report of FAS as an important target in GBM tumors. While the work is not in prostate, it arose specifically because of our prostate oriented research. The reference is listed below in the Reportable Outcomes section.

Key Research Accomplishments.

- Determination that FAS inhibitors induce ER stress.
- Increased cell killing when FAS inhibitors are combined with other ER stressing agents, including the FDA approved proteasome inhibitor that also induces ER stress.
- That ER stress can also affect FAS activity in tumor cells.
- Expression of FAS can be significantly increased by the c-src oncogene.
- Inhibition of the fatty acid synthesis pathway can inhibit src driven invasion.

Reportable Outcomes:

Abstracts

- Little, J.L., Wheeler F., Fels, D.R., Koumenis C. and Kridel S.J., Inhibition of FAS in tumor cells induces ER stress-dependent cell death, 97th Annual Meeting of the American Association for Cancer Research, Washington, D.C. April 1-5, 2006.

- Little, J.L., Wheeler F., Fels, D.R., Koumenis C. and Kridel S.J., Fatty acid synthase inhibitors induce ER stress-dependent cell death, 11th Prouts Neck Meeting in Prostate Cancer, Prouts Neck, Maine, November 2-5, 2006.

Publications

- Little, J.L., Wheeler F., Fels, D.R., Koumenis C. and Kridel S.J., (2006) Fatty acid synthase inhibitors induce ER stress in tumor cells, *Cancer Research,* Accepted for publication November 2006.

- W. Zhao, S. Kridel, A. Thorburn, M. Kooshki, J. Little, S. Hebbar and M. Robbins, (2006) Fatty acid synthase: a novel target for antiglioma therapy. *British Journal of Cancer* **95,** 869-878.

Aim 2: Orlistat complexes of FAS-TE. As described in the previous update, we have established protocols for the recombinant expression, purification and crystallization of human FAS-TE. By growing crystals of FAS-TE pre-derivatized with Orlistat, we have been able to observe two different views of Orlistat bound to the active site. We have shown for the first time that the enzymatic action of FAS-TE on Orlistat (Fig. 5, Orlistat/Palmitoyl Co-A figure) results in the cleavage of the -lactone ring, formation of a stable acyl-enzyme intermediate, and inhibition of the enzyme. These structures have now been fully refined and a manuscript describing the results is in preparation. A brief summary of our findings is given below.

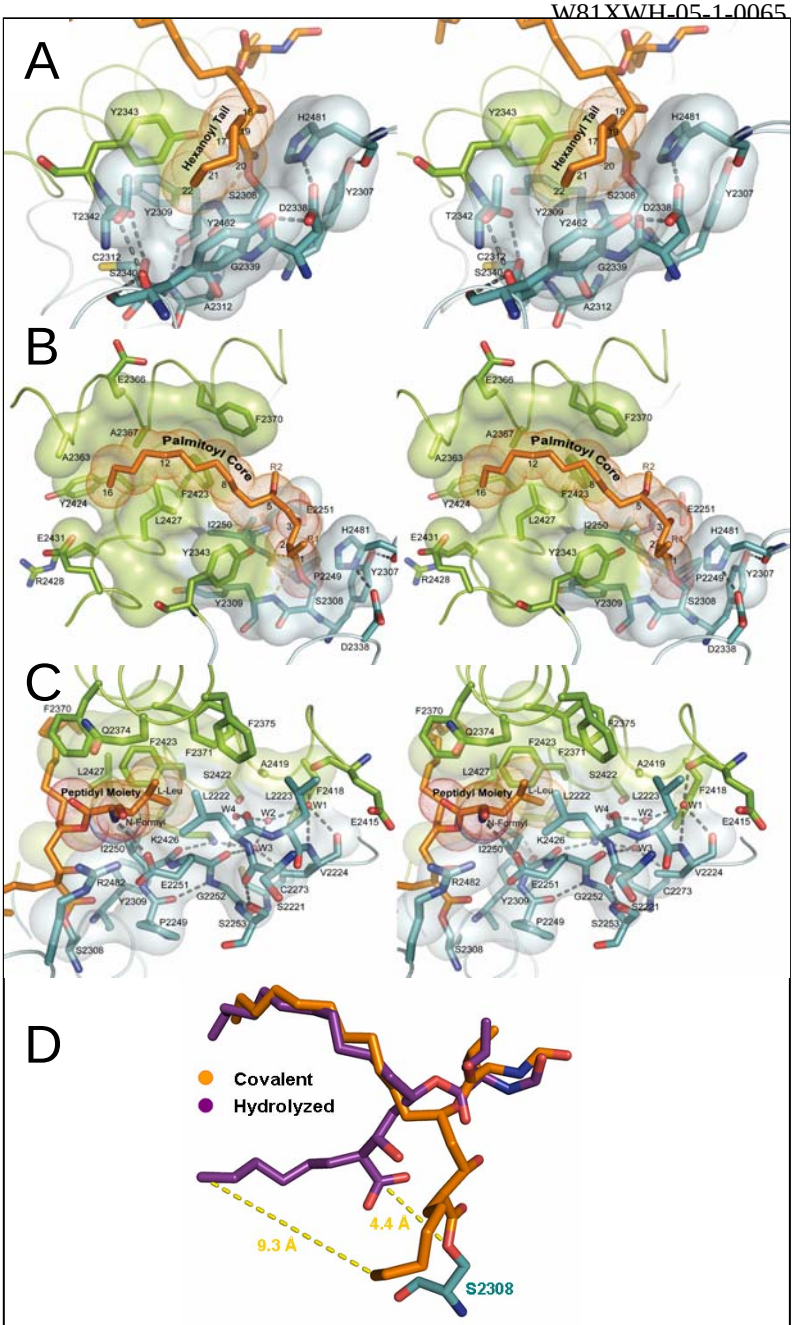

Figure 5. Molecular interactions of Orlistat with FAS-TE. (A) Stereo-images of the interactions of the hexanoyl tail adjacent to the catalytic triad. (B) Binding mode of the palmitic core. (C) Interaction of the peptidyl moiety. (D) Superposition of the covalent, Orilstat adduct and its hydrolyzed product.

A 2.3 Å dataset collected from a crystal grown over a two week period clearly shows the covalent adduct between Ser2308 and the C1 carbonyl group of the former β-lactone ring of Orlistat (Fig.5). This complex *(R_{work}/R_{free} = 20.4/26.4%)* provides the first rationale for the site of attack on the β-lactone ring and the unusual stability of the acyl-enzyme intermediate that results in inhibition. The attack of Ser2308 on the C1 atom over the C3 atom of Orlistat is consistent with the observed reactions with pancreatic lipase and chemical reactivity considerations (36). The stability of the intermediate appears to come from the extensive contacts of the lipophilic components of Orlistat to the enzyme surface (Fig. 5A & B). As a result the C3 hydroxyl oxygen atom and the nitrogen atom of the N-formyl moiety hydrogen bond to Glu2251 (Fig. 5C). These interactions are of particular importance since they most likely prevent the activation of a water molecule by His2481 that under normal catalysis would readily hydrolyze the intermediate. Moreover, this binding mode is different from the typical interactions of a carbonyl group within the oxyanion hole of α/β hydrolases including serine proteases (37-39). If the FAS-TE:Orlistat complex followed the latter contexts, the ester group would interact with the backbone nitrogen atoms of Ile2250 and Tyr2309.

A 1.95 Å structure of the Orlistat complex has also been determined from crystals that took several months to grow. In this complex the acyl-intermediate was hydrolyzed (Fig. 5D) (R_{work}/R_{free} = 19.2/24.7%). Hydrolysis of the ester bond resulted in a carboxyl group at C1. This group interacts through a water molecule

to the backbone nitrogen atoms of Ile2250 and Tyr2309 and the O^{γ} atom of Ser2308. Together these changes cause a significant shift of the inhibitor to the left when compared to the covalent adduct. Palmitate was proposed to partially bind in the interface cavity (40). In contrast, we observe that the fatty acid portion of Orlistat (extends off the C5 position) binds to what we have coined the "specificity channel" (Fig. 5B) and the N-formyl-Leu binds within the interface cavity (Fig. 5C). Several conserved residues from subdomain B (e.g. Phe2423, Tyr2424, and Leu2427) line the specificity channel. The binding of Orlistat to this channel is consistent with the observation that loop insertions in the α/β hydrolase fold in this region often modulate or mediate substrate binding (41). Experiments in the final year of funding will test the hypothesis that substrate binds in a similar manner to the active site of FAS-TE. This objective will be accomplished by an activity analysis of site-directed mutants of residues within the putative specificity channel and the structure determinations of the substrate and product complexes.

The new FAS-TE:Orlistat structures are a significant advance for the structure-based design of compounds to inhibit FAS for cancer treatment. For example, the N-formyl-Leu moiety may not completely fill the interface cavity (Fig. 5C). One can easily envision extending the chain further and to install functional groups that maximize interactions with the mixed hydrophobic/hydrophilic character of this cavity. Another intriguing possibility would be to modify the 6-carbon group that extends off of the C2 position ("hexanoyl tail") of Orlistat (Fig. 5A). We have already shown that treatment with Ebelactone B (EbeB) and not Ebelactone A (EbeA) leads to significant inhibition of FAS (42). EbeB contains an ethyl group at C2 while EbeA contains a methyl group. Therefore, it is clear that a minimum of a 2-carbon chain is necessary at this position. Moreover, modifying the C2 group to maximize a charge-charge interaction with Glu2431 and/or a pi-stacking interaction with Tyr2343 may be extremely beneficial for improving the selectivity of the compound for FAS.

Our current crystal structures only start to give us a picture of the potential interactions that may be necessary to exploit in order to generate drugs that specifically target prostate cancer cells. As a further step toward understanding the Orlistat scaffold, we will determine the binding mode of Orlistat to FAS-TE prior to the formation of the acyl-enzyme intermediate by using the Ser2308Ala mutant. This structure along with the others already determined will give three key snapshots of FAS-TE catalysis and inhibition: (i) binding of Orlistat prior to adduct formation, (ii) formation of the stable acyl-enzyme intermediate (i.e. the inhibited enzyme), and (iii) breakdown of covalent intermediate.

In summary, our structural work to date has resulted in several key observations. (i) Orlistat is in fact a substrate of FAS-TE. (ii) FAS-TE is inhibited by the formation of a stable acyl-enyzyme intermediate. (iii) Hydrolysis of the intermediate occurs slowly. (iv) Upon hydrolysis the binding mode of Orlistat shifts with respect to the catalytic triad. (v) The palmitate-like 16 carbon structure of Orlistat binds to an elongated hydrophobic channel that is exclusively generated by subdomain B. (vi) This binding mode is in stark contrast to the proposed binding mode of palmitoyl-CoA from a previous modeling/mutagenesis study. The manuscript reporting these finding is in preparation and will be submitted in December 2006.

Key Research Accomplishments:

- Determination of the crystal structures of Orlistat bound to human FAS-TE in two different binding modes, i.e. covalent and hydrolyzed.

Reportable Outcomes:

Abstracts:

- Pemble, C.P., Kridel, S.J., Lowther W.T. Thioesterase domain of human fatty acid synthase: structural insights into chain-length selectivity. Meeting of the American Crystallographic Association, Honolulu, Hawaii, July 22-26, 2006.

Oral Presentations:

- Pemble, C.P., Kridel, S.J., Lowther W.T., 36th Mid-Atlantic Macromolecular Crystallography Meeting (MAMC), Winston-Salem, NC, "Thioesterase domain of human fatty acid synthase: Structural and Insights into chain-length selectivity," June 2, 2006

Awards:

- Charles Pemble, Protein Data Bank Poster Prize, Meeting of the American Crystallographic Association, Honolulu, Hawaii, July 22-26, 2006.

References

1. Milgraum, L. Z., Witters, L. A., Pasternack, G. R., and Kuhajda, F. P. Enzymes of the fatty acid synthesis pathway are highly expressed in in situ breast carcinoma. Clinical Cancer Research, *3:* 2115-2120, 1997.
2. Swinnen, J. V., Van Veldhoven, P. P., Timmermans, L., De Schrijver, E., Brusselmans, K., Vanderhoydonc, F., Van de Sande, T., Heemers, H., Heyns, W., and Verhoeven, G. Fatty acid synthase drives the synthesis of phospholipids partitioning into detergent-resistant membrane microdomains. Biochem Biophys Res Commun, *302:* 898-903, 2003.
3. van der Sanden, M. H., Houweling, M., van Golde, L. M., and Vaandrager, A. B. Inhibition of phosphatidylcholine synthesis induces expression of the endoplasmic reticulum stress and apoptosis-related protein CCAAT/enhancer-binding protein-homologous protein (CHOP/GADD153). Biochem J, *369:* 643-650, 2003.
4. Ma, Y. and Hendershot, L. M. The unfolding tale of the unfolded protein response. Cell, *107:* 827-830, 2001.
5. Ma, Y. and Hendershot, L. M. The role of the unfolded protein response in tumour development: friend or foe? Nat Rev Cancer, *4:* 966-977, 2004.
6. Thupari, J. N., Landree, L. E., Ronnett, G. V., and Kuhajda, F. P. C75 increases peripheral energy utilization and fatty acid oxidation in diet-induced obesity. Proc Natl Acad Sci U S A, *99:* 9498-9502, 2002.
7. Schroder, M. and Kaufman, R. J. The mammalian unfolded protein response. Annu Rev Biochem, *74:* 739-789, 2005.
8. Koumenis, C., Naczki, C., Koritzinsky, M., Rastani, S., Diehl, A., Sonenberg, N., Koromilas, A., and Wouters, B. G. Regulation of protein synthesis by hypoxia via activation of the endoplasmic reticulum kinase PERK and phosphorylation of the translation initiation factor eIF2alpha. Mol Cell Biol, *22:* 7405-7416, 2002.
9. Xu, C., Bailly-Maitre, B., and Reed, J. C. Endoplasmic reticulum stress: cell life and death decisions. J Clin Invest, *115:* 2656-2664, 2005.
10. Harding, H. P., Zhang, Y., and Ron, D. Protein translation and folding are coupled by an endoplasmic-reticulum-resident kinase. Nature, *397:* 271-274, 1999.
11. Harding, H. P., Novoa, I., Zhang, Y., Zeng, H., Wek, R., Schapira, M., and Ron, D. Regulated translation initiation controls stress-induced gene expression in mammalian cells. Mol Cell, *6:* 1099-1108, 2000.

12. Cullinan, S. B., Zhang, D., Hannink, M., Arvisais, E., Kaufman, R. J., and Diehl, J. A. Nrf2 is a direct PERK substrate and effector of PERK-dependent cell survival. Mol Cell Biol, *23:* 7198-7209, 2003.
13. Cullinan, S. B. and Diehl, J. A. PERK-dependent activation of Nrf2 contributes to redox homeostasis and cell survival following endoplasmic reticulum stress. J Biol Chem, *279:* 20108-20117, 2004.
14. Shen, X., Ellis, R. E., Lee, K., Liu, C.-Y., Yang, K., Solomon, A., Yoshida, H., Morimoto, R., Kurnit, D. M., Mori, K., and Kaufman, R. J. Complementary Signaling Pathways Regulate the Unfolded Protein Response and Are Required for C. elegans Development. Cell, *107:* 893-903, 2001.
15. Tirasophon, W., Lee, K., Callaghan, B., Welihinda, A., and Kaufman, R. J. The endoribonuclease activity of mammalian IRE1 autoregulates its mRNA and is required for the unfolded protein response. Genes Dev, *14:* 2725-2736, 2000.
16. Calfon, M., Zeng, H., Urano, F., Till, J. H., Hubbard, S. R., Harding, H. P., Clark, S. G., and Ron, D. IRE1 couples endoplasmic reticulum load to secretory capacity by processing the XBP-1 mRNA. Nature, *415:* 92-96, 2002.
17. Lee, A. H., Iwakoshi, N. N., and Glimcher, L. H. XBP-1 regulates a subset of endoplasmic reticulum resident chaperone genes in the unfolded protein response. Mol Cell Biol, *23:* 7448-7459, 2003.
18. Sriburi, R., Jackowski, S., Mori, K., and Brewer, J. W. XBP1: a link between the unfolded protein response, lipid biosynthesis, and biogenesis of the endoplasmic reticulum. J. Cell Biol., *167:* 35-41, 2004.
19. Urano, F., Wang, X., Bertolotti, A., Zhang, Y., Chung, P., Harding, H. P., and Ron, D. Coupling of stress in the ER to activation of JNK protein kinases by transmembrane protein kinase IRE1. Science, *287:* 664-666, 2000.
20. Yoneda, T., Imaizumi, K., Oono, K., Yui, D., Gomi, F., Katayama, T., and Tohyama, M. Activation of caspase-12, an endoplastic reticulum (ER) resident caspase, through tumor necrosis factor receptor-associated factor 2-dependent mechanism in response to the ER stress. J Biol Chem, *276:* 13935-13940, 2001.
21. Menendez, J. A., Mehmi, I., Atlas, E., Colomer, R., and Lupu, R. Novel signaling molecules implicated in tumor-associated fatty acid synthase-dependent breast cancer cell proliferation and survival: Role of exogenous dietary fatty acids, p53-p21WAF1/CIP1, ERK1/2 MAPK, p27KIP1, BRCA1, and NF-kappaB. Int J Oncol, *24:* 591-608, 2004.
22. Okada, T., Kawano, Y., Sakakibara, T., Hazeki, O., and Ui, M. Essential role of phosphatidylinositol 3-kinase in insulin-induced glucose transport and antilipolysis in rat adipocytes. Studies with a selective inhibitor wortmannin. J. Biol. Chem., *269:* 3568-3573, 1994.
23. Gray, M. D., Mann, M., Nitiss, J. L., and Hendershot, L. M. Activation of the UPR is necessary and sufficient for reducing topoisomerase II {alpha} protein levels and decreasing sensitivity to topoisomerase targeted drugs. Mol Pharmacol, 2005.
24. Blais, J. D., Filipenko, V., Bi, M., Harding, H. P., Ron, D., Koumenis, C., Wouters, B. G., and Bell, J. C. Activating transcription factor 4 is translationally regulated by hypoxic stress. Mol Cell Biol, *24:* 7469-7482, 2004.
25. Wouters, B. G., van den Beucken, T., Magagnin, M. G., Koritzinsky, M., Fels, D., and Koumenis, C. Control of the hypoxic response through regulation of mRNA translation. Semin Cell Dev Biol, *16:* 487-501, 2005.
26. Feng, B., Yao, P. M., Li, Y., Devlin, C. M., Zhang, D., Harding, H. P., Sweeney, M., Rong, J. X., Kuriakose, G., Fisher, E. A., Marks, A. R., Ron, D., and Tabas, I. The endoplasmic reticulum is the site of cholesterol-induced cytotoxicity in macrophages. Nat Cell Biol, *5:* 781-792, 2003.
27. Harding, H. P., Zhang, Y., Khersonsky, S., Marciniak, S., Scheuner, D., Kaufman, R. J., Javitt, N., Chang, Y. T., and Ron, D. Bioactive small molecules reveal antagonism between the integrated stress response and sterol-regulated gene expression. Cell Metab, *2:* 361-371, 2005.
28. van der Sanden, M. H. M., Meems, H., Houweling, M., Helms, J. B., and Vaandrager, A. B. Induction of CCAAT/Enhancer-binding Protein (C/EBP)-homologous Protein/Growth Arrest and DNA Damage-inducible Protein 153 Expression during Inhibition of Phosphatidylcholine Synthesis Is Mediated via

Activation of a C/EBP-activating Transcription Factor-responsive Element. J. Biol. Chem., *279:* 52007-52015, 2004.
29. Nawrocki, S. T., Carew, J. S., Pino, M. S., Highshaw, R. A., Dunner, K., Jr., Huang, P., Abbruzzese, J. L., and McConkey, D. J. Bortezomib Sensitizes Pancreatic Cancer Cells to Endoplasmic Reticulum Stress-Mediated Apoptosis. Cancer Res, *65:* 11658-11666, 2005.
30. Fribley, A., Zeng, Q., and Wang, C.-Y. Proteasome Inhibitor PS-341 Induces Apoptosis through Induction of Endoplasmic Reticulum Stress-Reactive Oxygen Species in Head and Neck Squamous Cell Carcinoma Cells. Mol. Cell. Biol., *24:* 9695-9704, 2004.
31. Swinnen, J. V., Esquenet, M., Goossens, K., Heyns, W., and Verhoeven, G. Androgens stimulate fatty acid synthase in the human prostate cancer cell line LNCaP. Cancer Res, *57:* 1086-1090, 1997.
32. Van de Sande, T., De Schrijver, E., Heyns, W., Verhoeven, G., and Swinnen, J. V. Role of the phosphatidylinositol 3'-kinase/PTEN/Akt kinase pathway in the overexpression of fatty acid synthase in LNCaP prostate cancer cells. Cancer Res, *62:* 642-646, 2002.
33. Menendez, J. A., Vellon, L., Mehmi, I., Oza, B. P., Ropero, S., Colomer, R., and Lupu, R. Inhibition of fatty acid synthase (FAS) suppresses HER2/neu (erbB-2) oncogene overexpression in cancer cells. Proc Natl Acad Sci U S A, *101:* 10715-10720, 2004.
34. Seals, D. F., Azucena, E. F., Jr., Pass, I., Tesfay, L., Gordon, R., Woodrow, M., Resau, J. H., and Courtneidge, S. A. The adaptor protein Tks5/Fish is required for podosome formation and function, and for the protease-driven invasion of cancer cells. Cancer Cell, *7:* 155-165, 2005.
35. Rossi, S., Graner, E., Febbo, P., Weinstein, L., Bhattacharya, N., Onody, T., Bubley, G., Balk, S., and Loda, M. Fatty acid synthase expression defines distinct molecular signatures in prostate cancer. Mol Cancer Res, *1:* 707-715, 2003.
36. Drahl, C., Cravatt, B. F., and Sorensen, E. J. Protein-reactive natural products. Angew Chem Int Ed Engl, *44:* 5788-5809, 2005.
37. Dodson, G. and Wlodawer, A. Catalytic triads and their relatives. Trends Biochem Sci, *23:* 347-352, 1998.
38. Kraut, J. Serine proteases: structure and mechanism of catalysis. Annu Rev Biochem, *46:* 331-358, 1977.
39. Katona, G., Wilmouth, R. C., Wright, P. A., Berglund, G. I., Hajdu, J., Neutze, R., and Schofield, C. J. X-ray structure of a serine protease acyl-enzyme complex at 0.95-A resolution. J Biol Chem, *277:* 21962-21970, 2002.
40. Chakravarty, B., Gu, Z., Chirala, S. S., Wakil, S. J., and Quiocho, F. A. Human fatty acid synthase: structure and substrate selectivity of the thioesterase domain. Proc Natl Acad Sci U S A, *101:* 15567-15572, 2004.
41. Nardini, M. and Dijkstra, B. W. Alpha/beta hydrolase fold enzymes: the family keeps growing. Curr Opin Struct Biol, *9:* 732-737, 1999.
42. Kridel, S. J., Axelrod, F., Rozenkrantz, N., and Smith, J. W. Orlistat is a novel inhibitor of fatty acid synthase with antitumor activity. Cancer Res, *64:* 2070-2075, 2004.

Inhibition of Fatty Acid Synthase Induces ER Stress in Tumor Cells.

Joy L. Little, [1] Frances B. Wheeler, [1] Diane R. Fels, [1] Constantinos Koumenis, [1,2,3] and Steven J. Kridel [1]

[1] Department of Cancer Biology, [2] Department of Radiation Biology, [3] Department of Neurosurgery, Comprehensive Cancer Center, Wake Forest University School of Medicine, Winston-Salem, NC.

Requests for Reprints: Steven J. Kridel, Department of Cancer Biology, Comprehensive Cancer Center, Wake Forest University School of Medicine, Medical Center Boulevard, Winston-Salem, NC, 27157. Phone: (336)716-7299, E-mail: skridel@wfubmc.edu

Grant Support: This research was supported by the Department of Defense Prostate Cancer Research Program under award number (W81XWH-05-1-0065) to S.K. Views and opinions of, and endorsements by the author(s) do not reflect those of the US Army or the Department of Defense. C.K. is supported by grant CA94214.

Note: C. Koumenis is currently at the Department of Radiation Oncology, University of Pennsylvania School of Medicine, Philadelphia, PA.

Running title: Fatty acid synthase inhibitors induce ER stress in tumor cells

Key words: fatty acid synthase, ER stress, apoptosis, orlistat, C75

Abstract

Fatty acid synthase (FAS), the cellular enzyme that synthesizes palmitate, is expressed at high levels in tumor cells and is vital for their survival. Through synthesis of palmitate, FAS primarily drives the synthesis of phospholipids in tumor cells. In this study, we tested the hypothesis that the FAS inhibitors induce endoplasmic reticulum (ER) stress in tumor cells. Treatment of tumor cells with FAS inhibitors induces robust PERK-dependent phosphorylation of the translation initiation factor eIF2α and concomitant inhibition of protein synthesis. PERK deficient transformed mouse embryonic fibroblasts (MEFs) and HT-29 colon carcinoma cells that express a dominant negative PERK (ΔC-PERK) are hypersensitive to FAS inhibitor-induced cell death. Pharmacological inhibition of FAS also induces processing of XBP-1, indicating that the IRE1 arm of the ER stress response is activated when FAS is inhibited. Induction of ER stress is further confirmed by increased expression of the ER stress-regulated genes CHOP, ATF4 and GRP78. FAS inhibitor-induced ER stress is activated prior to the detection of caspase 3 and PARP cleavage, primary indicators of cell death, and orlistat-induced cell death is rescued by co-incubation with the global translation inhibitor cycloheximide. Lastly, FAS inhibitors cooperate with the ER stress inducer thapsigargin to enhance tumor cell killing. These results provide the first evidence that FAS inhibitors induce ER stress and establish an important mechanistic link between FAS activity and ER function.

Introduction

Fatty acid synthase (FAS) is a multifunctional enzyme that catalyzes the terminal steps in the synthesis of the 16-carbon fatty acid palmitate in cells (1, 2). In normal tissue the FAS expression levels are relatively low as fatty acid is generally supplied by dietary fatty acids. On the other hand, FAS is expressed at significantly higher levels in many tumors including those of the prostate, breast, colon, ovary and others (3-5). This expression profile suggests that tumors require higher levels of fatty acids than can be supplied from circulation. Several reports have demonstrated that FAS expression levels correlate with tumor progression, aggressiveness and metastasis (5-7). In fact, FAS expression levels are predictive of the progression from organ-confined prostate cancer to metastatic prostate cancer (6), indicating that FAS provides a metabolic advantage to tumor cells. Because of the strong link between FAS expression and cancer, FAS has become an attractive target for therapeutic intervention.

The functional connection between FAS and tumor progression has been provided by the discovery and design of small molecule drugs that inhibit the catalytic activity of FAS (8, 9). Cerulenin and C75, which target the keto-acyl synthase domain of FAS, were the first small molecules to be described as inhibitors of FAS activity in human tumor cells. These pharmacological agents inhibit FAS activity and induce cell death in many tumor cell lines *in vitro* (5, 7). The compounds are also effective at inhibiting the growth of human tumor xenografts *in vivo* and have chemopreventive abilities (10-12). We were the first to describe orlistat as an inhibitor of the thioesterase domain of FAS (13). Orlistat inhibits FAS activity and induces cell death in a variety of tumor cell lines and is able to effectively inhibit the growth of prostate tumor xenografts in mice (13-15). The data linking FAS function and tumor cell survival

emphasizes the relevance of FAS as an attractive anti-tumor target. The importance of fatty acid synthesis in tumor cells is further underscored by data demonstrating that pharmacological and genetic inhibition of two upstream enzymes in the fatty acid synthesis pathway, ATP citrate lyase (ACL) and acetyl CoA carboxylase (ACC), also induces cell death in tumor cell lines (16-18).

Because FAS is a target for therapeutic intervention, it is important to fully understand the role of FAS in tumor cells as well as the anti-tumor effects of FAS inhibitors. Given that the endoplasmic reticulum (ER) is the major site for lipid synthesis in cells, it is not surprising that previous studies have identified a link between pathways that regulate lipid synthesis and the ER stress response (19-21). Fatty acid synthesis in general, and FAS activity in particular, drives phospholipid synthesis which primarily occurs in the ER (22). Because of the direct connection between FAS activity and phospholipid synthesis, we tested the hypothesis that pharmacological blockade of FAS activity might induce ER stress in tumor cells (22). The data presented herein demonstrates for the first time that inhibition of FAS induces ER stress specifically in a variety of tumor cells and not in normal cells. Importantly, we also demonstrate that FAS inhibitors cooperate with a known ER stress inducer, thapsigargin, to induce cell death. The data also provide evidence that FAS inhibitors might be combined with PERK inhibitors to more effectively treat cancer. The evidence suggests that increased FAS expression in tumor cells is important for ER function to maintain membrane biogenesis and suggests a role for ER stress in the anti-tumor effects of FAS inhibitors.

Experimental procedures

Materials. The PC-3, DU145, HT-29, HeLa, and FS-4 cell lines were obtained from American Type Culture Collection (Manassas, VA). Cell culture medium and supplements were from Invitrogen (Carlsbad, CA). Antibodies against eIF2α, phospho-eIF2α, cleaved caspase 3, and cleaved PARP were from Cell Signaling Technologies (Beverly, MA). Antibody against fatty acid synthase was from BD Transduction Labs (San Diego, CA). Antibody against β-tubulin was from NeoMarkers (Fremont, CA). Trizol was from Invitrogen (Carlsbad, CA). Avian Myleoblastosis Virus (AMV) Reverse Transcriptase and Taq Polymerase were from Promega (Madison, WI). ^{35}S-methionine and ^{14}C-acetate were purchased from GE Healthcare (formerly Amersham Biosciences, Piscataway, NJ). Oligonucleotides were synthesized by Integrated DNA Technologies (Coralville, IA), except for those designed for siRNA which were synthesized by Dharmacon (Lafayette, Co). All other reagents were purchased from Sigma (St. Louis, MO), Calbiochem (San Diego, CA) or BioRad (Hercules, CA).

Cell culture and drug treatments. Prostate tumor cell lines were maintained in RPMI 1640 supplemented with 10% fetal bovine serum at 37°C and 5% CO_2. Wild-type and *PERK*$^{-/-}$ mouse embryonic fibroblasts (MEFs), obtained from David Ron (New York University), HeLa cervical cancer cells, and FS-4 human foreskin fibroblasts were maintained in DMEM-high glucose supplemented with 10% fetal bovine serum. HT-29 colon carcinoma cells were maintained in McCoy's 5A media supplemented with 10% FBS. HT-29 cells expressing the pBabe-puro empty vector or the pBabe-puro-ΔC-PERK construct were maintained with 1 μg/ml puromycin and supplemented with 20% FBS, non-essential amino acids and 2-mercaptoethanol. Cells were treated for the indicated times and drug concentrations as indicated. Orlistat was extracted from

capsules in EtOH as described previously and stored at -80°C (13). Further dilutions were made in dimethyl sulfoxide (DMSO).

Generation of ΔC-PERK expressing cells. To generate human tumor cells with deficient PERK signaling, HT-29 cells seeded in 6-well plates were transfected with 1 μg of pBabe-puro or pBabe-puro-ΔC-PERK using Lipofectamine (Invitrogen). These plasmids have been described previously (23). Stable populations of each construct were selected by incubating transfected cells with 3 μg/ml puromycin for 48 hours. The transfected cell populations were then maintained in 1 μg/ml puromycin for subsequent experiments in the media described above.

Immunoblot analysis. Cells were harvested after the indicated treatments, washed with ice-cold phosphate-buffered saline, and lysed in buffer containing 1% Triton X-100 and a complete protease, kinase, and phosphatase inhibitor cocktail. Protein samples were electrophoresed through 7.5%, 10% or 12% SDS-polyacrylamide gels and transferred to nitrocellulose, except for blots to detect phospho-eIF2α and eIF2α, which were transferred to Immobilon-P membrane (PVDF). Immunoreactive bands were detected by enhanced chemiluminescence (Perkin Elmer).

Metabolic labeling of protein and fatty acid synthesis. To measure fatty acid synthesis, 1×10^5 cells per well were seeded in 24-well plates. Cells were treated with C75 (10 μg/ml), orlistat (25, 50 μM), or cerulenin (5, 10 μg/ml) for 2 hours. ^{14}C-acetate (1 μCi) was added to each well for two hours. Cells were collected, washed and lipids were extracted and quantified as previously described (13). To measure new protein synthesis, PC-3 cells were seeded in 6-well plates. Orlistat (50 μM) and thapsigargin (1 μM) were added for the indicated times. After incubation

with orlistat or thapsigargin, the cells were switched to methionine deficient medium while maintaining the drug concentrations. Methionine deficient medium supplemented with 100 μCi/ml ^{35}S-methionine was added to the cells for thirty minutes to label newly synthesized proteins. After the labeling period, cells were washed, lysed and samples were resolved by electrophoresis through a 10%-SDS-polyacrylamide gel. The gel was then stained with Coomassie, dried and relative protein synthesis of each sample was quantified after scanning with a Typhoon 9210 (Amersham) using ImageQuant software.

Clonogenic survival assays. Cells were plated in 6-well plates at low density depending on the individual cell type. PC-3 cells were plated at a density of 800 cells per well, except for the experiment combining C75 with thapsigargin, for which PC-3 cells were plated at 3000 cells per well. HT-29 and MEF cells were plated at a density of 400 cells per well. Human tumor cells were plated 48 hours prior to each experiment, while MEFs were plated 24 hours prior to treatment. Fresh medium containing the indicated drugs was added at the indicated concentrations for 12-20 hours as indicated. The media was then removed, the wells were washed and fresh medium was added. Plates were incubated until macroscopic colonies were formed. To visualize colonies the wells were washed twice with ice-cold phosphate-buffered saline and fixed for 10 minutes with a 10% methanol, 10% acetic acid solution. Colonies were stained with a 0.4% crystal violet, 20% methanol solution for 10 minutes. The crystal violet solution was removed, the wells were washed with water to remove excess dye, and dried at room temperature overnight. Colonies were quantified by counting and by solubilization in 33% acetic acid followed by spectrophotometric analysis at 540 nM. Survival of treated cells was

normalized relative to vehicle treated cells and statistical significance was determined by two-tailed Student's *t* tests.

Detection of XBP-1 splicing and ATF4, GRP78, CHOP, and GADD34 expression. Cells were exposed to the various drug treatments or transfected with siRNA for the indicated times. Total RNA was isolated from cells using TRIzol according to the manufacturer's directions. cDNA was generated from 2 μg of total RNA using AMV-reverse transcriptase. XBP-1 was amplified by polymerase chain reaction (PCR) with Taq polymerase using the oligonucleotides AAACAGAGTAGCAGCTCAGACTGC (sense) and TCCTTCTGGGTAGACCTCTGGGAG (antisense). The XBP-1 products were resolved on 2% Tris-acetate-EDTA agarose gels and imaged on the Typhoon 9210 at 610nm. The expression of CHOP, ATF4, GRP78, and GADD34 was determined by semi-quantitative PCR using RNA collected as described above. Multiple cycles were tested for each gene to determine the optimum cycles in the linear range. The oligonucleotide sequences used were: CHOP, CAGAACCAGCAGAGGTCACA and AGCTGTGCCACTTTCCTTTC; GRP78, CTGGGTACATTTGATCTGACTGG and GCATCCTGGTGGCTTTCCAGCCATTC; ATF4, CTTACGTTGCCATGATCCCT and CTTCTGGCGGTACCTAGTGG; and GADD34, GTGGAAGCAGTAAAAGGAGCAG and CAGCAACTCCCTCTTCCTCG. The CHOP, GRP78 and ATF4 products were resolved on 1% Tris-acetate-EDTA agarose gels and imaged on the Typhoon 9210 at 610nm.

Suppression of FAS expression with siRNA. A paired siRNA oligonucleotide against the FAS gene (FAS1 sense, GUAGGCCUUCCACUCCUAUU) and one siRNA against luciferase as a negative control (Luc sense, CUUACGUGAUACUUCGAUU) were designed and synthesized

by Dharmacon. The individual siRNAs (30 nM) were transfected into cells at plating with siPORT *NeoFX* transfection reagent (Ambion) according to manufacturers instructions. Cells were collected at indicated times after transfection then harvested for RNA to perform RT-PCR or protein for immunoblot analysis.

Results

Pharmacological inhibition of FAS induces phosphorylation of eIF2α in tumor cells. Several studies have demonstrated that lipid composition is important for maintaining ER function (19-21, 24, 25). Other studies have demonstrated that FAS drives phospholipid synthesis in tumor cells (22). Because of this fact, we hypothesized that FAS inhibitors might induce ER stress. One hallmark of ER stress is the PERK-dependent phosphorylation of the translation initiation factor eIF2α. We first examined the phosphorylation status of eIF2α in cells treated with three different pharmacological inhibitors of FAS (Figure 1A). PC-3 cells were treated with orlistat (12.5-50 μM, left) or cerulenin (5 or 10 μg/ml, middle) for 16 hours, or C75 (10 μg/ml) for 8-24 hours (right). Each FAS inhibitor induced robust phosphorylation of eIF2α at each concentration after 16 hours of treatment, as did thapsigargin (data not shown). All three inhibitors induce eIF2α phosphorylation, similarly, regardless of tumor cell type tested (data not shown). Likewise, fatty acid synthesis was inhibited to similar degrees by each treatment, as measured by ^{14}C-acetate incorporation into total cellular lipids (Figure 1B, left). Because phosphorylation of eIF2α leads to inhibition of protein synthesis, we performed a ^{35}S-methionine labeling experiment to measure levels of newly synthesized proteins in cells treated with orlistat. PC-3 cells were treated with orlistat (50 μM) for 12 and 24 hours or thapsigargin (1 μM) as a positive control for 1 hour (Figure 1B, right). Orlistat treatment reduced protein synthesis by 56% after 12 hours and by 73% at 24 hours, similar to treatment with thapsigargin. Therefore, orlistat treatment is sufficient to induce phosphorylation of eIF2α and subsequently inhibit protein synthesis. To further confirm our findings, a genetic approach was also used to inhibit FAS expression. PC-3 cells were transfected with FAS-specific siRNA or siRNA against luciferase as a negative control. Immunoblot analysis demonstrated a nearly 70% reduction of

FAS protein in the samples 48 hours after transfection which continued through 72 hours (Figure 1C). Consistent with our findings using pharmacological inhibitors, reduction of FAS expression levels resulted in the detection of significant levels of phosphorylated eIF2α at 72 hours (Figure 1C). Conversely, treatment of normal human foreskin FS-4 fibroblasts with the FAS inhibitor orlistat did not result in phosphorylation of eIF2a (Figure 1D). Collectively these data indicate that eIF2α phosphorylation induced by FAS inhibition is, indeed, specific to both FAS and tumor cells.

PERK mediates eIF2α phosphorylation in response to orlistat treatment. There are four known eIF2α kinases: PERK, GCN2, PKR and HRI; but PERK is the kinase that phosphorylates eIF2α during the ER stress response (26). To determine whether PERK is the kinase responsible for the phosphorylation eIF2α in response to FAS inhibition, wild-type and $PERK^{-/-}$ mouse embryonic fibroblasts (MEFs) transformed with $Ki\text{-}Ras^{V12}$ were obtained and tested for their sensitivity to orlistat (27). The wild-type and $PERK^{-/-}$ MEFs were treated with orlistat (12.5 μM) for 8, 16 and 24 hours (Figure 2A) or treated with thapsigargin (1 μM) for 1 hour (data not shown). In the wild-type MEFs, orlistat induced phosphorylation of eIF2α within 8 hours (Figure 2A), consistent with our findings in prostate tumor cell lines (Figure 1A). On the other hand, no significant phosphorylation of eIF2α was evident during the same time course of orlistat treatment in the PERK-deficient cells (Figure 2A). As expected, thapsigargin only induced phosphorylation of eIF2α in the wild-type and not the $PERK^{-/-}$ MEFs (data not shown). These data indicate that FAS inhibition results in PERK-dependent phosphorylation of eIF2α.

It has been demonstrated that PERK deficient cells are hypersensitive to ER stress-induced apoptosis (28). Because of this, we tested whether *PERK*$^{-/-}$ MEFs were hypersensitive to orlistat-induced cell death using clonogenic survival assays. Wild-type and *PERK*$^{-/-}$ MEFs were treated with vehicle, orlistat (25 μM) or thapsigargin (100 nM) for 16 hours (Figure 2B). As expected, the *PERK*$^{-/-}$ MEFs were hypersensitive to thapsigargin-induced cell death as demonstrated by a three-fold decrease in clonogenic survival ($p<0.005$). Similarly, the *PERK*$^{-/-}$ MEFs demonstrated hypersensitivity to orlistat treatment, showing reduced clonogenic survival of wild-type transformed MEFs to 70% of vehicle treated cells. On the other hand, clonogenic survival was decreased nearly four-fold to less than 20% ($p<0.005$) in the *PERK*$^{-/-}$ MEFs following orlistat treatment. These data indicate that inhibition of FAS activity induces ER stress which is exacerbated by loss of PERK.

To further support the results obtained in MEFs, we generated stable populations of HT-29 colon carcinoma cells transfected with a dominant negative PERK construct that lacks the kinase domain (ΔC-PERK) or the corresponding empty vector (23). These cells were seeded at low density and treated with C75 (9 μg/ml), orlistat (25 μM), or thapsigargin (10nM) to assess clonogenic survival. As expected, the HT-29 ΔC-PERK cells were hypersensitive to thapsigargin as demonstrated by a nearly three-fold reduction in clonogenic survival (Figure 2C, $p<0.005$). Similarly, the HT-29 ΔC-PERK cells were also hypersensitive to both orlistat and C75 compared to the empty-vector transfected cells. Clonogenic survival was reduced more than two-fold in C75 treated cells and nearly four-fold in orlistat treated cells (Figure 2C, $p<0.005$). These results confirm that PERK function is important for an adaptive response in tumor cells when FAS activity is inhibited.

Treatment with orlistat induces processing of XBP-1. In addition to the PERK-regulated arm, the ER stress response can also be mediated by IRE1, a kinase with endonuclease activity that facilitates splicing of X-box binding protein-1 (XBP-1) mRNA to yield the splice variant XBP-1(s) during ER stress (29). To determine whether pharmacological inhibition of FAS also activates the IRE1 pathway, the status of XBP-1 mRNA was assessed by RT-PCR using oligonucleotides that flank the splice site in the XBP-1 mRNA. Total RNA was collected from PC-3 cells treated with orlistat (50 μM) for 8-24 hours (Figure 3A) or with cerulenin (5 or 10 μg/ml) for 16 hours (Figure 3B). Thapsigargin treatment resulted in a loss of the 473 bp product associated with un-spliced XBP-1 and the appearance of the processed 447 bp form associated with XBP-1(s) that is produced only in response to ER stress (Figure 3A). Similarly, orlistat treatment resulted in the appearance of the 447 bp XBP-1(s) product in as few as 8 hours with maximum processing by 16 hours (Figure 3A). Cerulenin also induced processing of XBP-1 (Figure 3B). To further confirm the role of FAS inhibition in the processing of XBP-1 to XBP-1(s), HeLa cells were transfected with FAS-specific siRNA or siRNA against luciferase as a negative control and collected for RT-PCR (Figure 3C). The 447 bp fragment that corresponds to the ER stress specific XBP-1(s) product was detected at 72 hours in the FAS specific siRNA samples. While PC-3 cells exhibit XBP-1 splicing after both orlistat and thapsigargin treatment, FS-4 cells exhibited only minor induction of XBP-1 and no splicing in response to orlistat (Figure 3D). These results suggest that the IRE1 pathway of the ER stress response is activated in parallel to the PERK pathway when FAS is inhibited in tumor cells.

Inhibition of FAS activity induces expression of ER stress regulated genes. Activation of the ER stress response induces the expression of a number of genes associated with adaptation and cell death, including CHOP, GRP78 and ATF4. CHOP has been implicated in ER stress-dependent apoptosis and *CHOP*$^{-/-}$ cells are mildly resistant to apoptosis following treatment with ER stressing agents (30). The mRNA expression of CHOP is induced in DU145 cells treated with orlistat (50 μM) or C75 (9 μg/ml) (Figure 4A). Similar effects were seen in PC-3 cells (data not shown). CHOP mRNA expression was also induced following siRNA-mediated knockdown of FAS expression in PC-3 cells (Figure 4B). Increased mRNA expression of CHOP may indicate that ER stress could play a role in cell death induced by FAS inhibition (30). The mRNA expression of GRP78, an ER stress regulated chaperone, is also induced in orlistat treated cells (Figure 4C) (31). Furthermore, mRNA expression of the transcription factor ATF4, which is dependent on eIF2α phosphorylation, is also induced by orlistat treatment (Figure 4C). Collectively, the data in Figures 1-4 demonstrate that FAS inhibitors induce the ER stress response.

ER stress is an early event in cells treated with FAS inhibitors. To determine whether phosphorylation of eIF2α and subsequent indications of the ER stress response events coincide or precede cell death induced by FAS inhibition, we analyzed the temporal phosphorylation of eIF2α and markers of caspase activity and cell death. In PC-3 cells treated with orlistat, phosphorylation of eIF2α was evident at 16 hours of treatment, while significant cleavage of caspase 3 and PARP are not detectable until 24 and 48 hours, respectively, consistent with previous reports (13). These data indicate that the ER stress response is induced prior to caspase 3 activation and PARP cleavage. These data are further supported by the timeline of XBP-1

processing following orlistat treatment (Figure 3A). Previous studies have demonstrated that inhibition of protein translation with cycloheximide can ameliorate the effects of ER stress, likely by decreasing protein burden on the ER (28). Clonogenic survival assays and immunoblot analysis were performed in PC-3 cells treated with vehicle control, cycloheximide (CHX, 1 μg/ml), orlistat (25 μM), or orlistat with CHX (Figure 5B and C). Cycloheximide treatment rescued clonogenic survival of PC-3 cells treated with orlistat (Figure 5B), and also inhibited orlistat induced phosphorylation of eIF2α (Figure 5C). These data are consistent with previous reports on the protective effect of cycloheximide on cells under ER stress and suggest that reduced protein burden on the ER or reduced expression of a specific pro-apoptotic factor could be responsible.

Cooperation between FAS inhibitors and thapsigargin. At least one study has demonstrated that ER stress can have a negative effect on the activity of chemotherapeutic drugs (32). To determine the effect of ER stress on FAS inhibitor-induced cell death, clonogenic survival assays, immunoblot, and RT-PCR analysis were performed on tumor cells treated with orlistat or C75 in combination with the ER stressing agent thapsigargin (Figure 6A and B). Lower doses of FAS inhibitors and thapsigargin were used to achieve reduced cell kill by either single agent in order to maximize the effect of the combination of the two drugs. PC-3 cells were seeded at low density and treated with C75 (9 μg/ml), thapsigargin (25 nM), or the combination of both for 12 hours and assayed for clonogenic survival. The clonogenic survival of cells treated with the combination of drugs was significantly reduced compared with either agent alone (Figure 6A, left). This coincides with immunoblot data demonstrating that levels of cleaved PARP are highest in lysates from cells treated with both drugs (Figure 6A, top right). Interestingly, while

both C75 and thapsigargin induced phosphorylation of eIF2α separately, the level of phosphorylated eIF2α was significantly reduced in cells treated with the two agents combined, with no change in total eIF2α levels (Figure 6A, top right). This data suggests that the combined agents facilitated a more rapid progression of the ER stress response and induction of the GADD34 feedback loop (33). In support of this, mRNA expression of GADD34 is increased in PC-3 cells treated with both agents, as compared with either agent alone (Figure 6A, bottom right). Confirming that the effects of this combination of drugs is not cell-type-specific, clonogenic survival was assessed in HT-29 cells treated with one of two combinations: either 1) orlistat (25 μM), thapsigargin (25 nM) or the combination of both for 12 hours (Figure 6B, left); or, 2) C75 (9 μg/ml), thapsigargin (25 nM) or the combination of both for 12 hours (Figure 6B, right). While the clonogenic survival only indicates an additive interaction, these data, importantly, demonstrate that ER stress does not inhibit the actions of FAS inhibitors and may actually enhance their efficacy.

Discussion

The ER stress response is a choreographed series of cellular events activated by specific insults that result in altered ER function (34). The combined effect of this response is activation of genes that are specifically expressed to engage an adaptation protocol. Upon prolonged stress, the adaptation mechanism of the ER stress response saturates, thus, activating cell death. Several studies have developed important connections between lipid synthesis pathways and the ER stress response (19-21, 35). Inhibition of phospholipid synthesis, especially that of phosphatidylcholine (PtdCho), induces ER stress-related pathways (20). Similarly, altering phospholipid metabolism by manipulation of phospholipase activity amplifies the ER stress response in β-cells (36). In addition, the accumulation of the G_{M1}-ganglioside activates the ER stress response in neurons, indicating that sphingolipid levels are also important for regulating ER function (35). Recent studies have demonstrated that cholesterol-induced apoptosis in macrophages is triggered by ER stress induction, and small molecule inhibitors of cholesterol synthesis activate the integrated stress response (24, 25). There are also direct links between the individual ER stress components and lipid synthesis pathways. For instance, overexpression of the ER stress specific XBP-1(s) expands ER volume by increasing the activity of enzymes responsible for PtdCho synthesis (37, 38). Moreover, mice that are null for XBP-1 have underdeveloped ER (26, 39). Collectively, these data demonstrate that lipid and sterol levels are important for maintaining ER function.

Because FAS inhibitors are being developed as anti-tumor agents, it is important to understand the effects these drugs have on both normal and tumor cells. The evidence here demonstrates that FAS inhibitors induce the ER stress response in a variety of tumor cells, but

not in normal cells. A model summarizing these data is presented in Figure 6C. Our results suggest that in a proliferating tumor cell FAS activity drives phospholipid synthesis which facilitates ER homeostasis and function. When FAS activity is inhibited in tumor cells, the result is PERK-dependent phosphorylation of eIF2α, a concomitant attenuation of protein synthesis and the IRE1-mediated processing of XBP-1. Interestingly, phosphorylation of eIF2α persists for as long as 48 hours with no attenuation (Figure 5A), suggesting that protein phosphatase 1 activity is not activated or that GADD34 is not induced as is evidenced by lack of expression in Figure 6A. Downstream of PERK and IRE1 activation, inhibiting FAS activity also induces mRNA expression of canonical markers of the ER stress response pathway including CHOP, GRP78 and ATF4. The precise role of these players has not been determined in cells that have been treated with FAS inhibitors. However, it has previously been shown that ATF4 acts to protect cells from ER generated reactive oxygen species (40). Another report demonstrated that siRNA-mediated knockdown of FAS or ACC in breast cancer cells results in cell death that is mediated by reactive oxygen species and attenuated by supplementation with the antioxidant vitamin E, which suggests that the ER stress response in general, and ATF4 expression specifically, may be a response to changes in the redox status of FAS inhibitor treated cells (18). These data are consistent with the hypothesis that the ER stress response initially acts to protect cells from FAS inhibitors, but do not rule out that ER stress could also facilitate cell death after prolonged death.

It is interesting to note that several indicators of ER stress, including phosphorylation of eIF2α, inhibition of protein synthesis, and XBP-1 processing are detected well before canonical hallmarks of apoptosis, cleaved caspase 3 and cleaved PARP. This indicates that the ER may be an early sensor of fatty acid and phospholipid levels in tumor cells. When the ER stress response

is unable to fully restore ER function perturbed by FAS inhibition, it is possible that this leads to the initiation of a cell death program. Consistent with this notion, cycloheximide is able to inhibit orlistat induced cell death and phosphorylation of eIF2α. These data do not conflict with previous reports demonstrating that FAS inhibitors activate the intrinsic cell death pathway and that ceramide accumulation contributes to FAS inhibitor induced cell death (34, 41). In fact, a previous study demonstrated that ceramide accumulation is also associated with thapsigargin induced ER stress and apoptosis (36). It is possible that FAS inhibitor induced ER stress may result in ceramide accumulation that is important in for cell death; however, the relationship between FAS inhibition, ER stress, and subsequent downstream events remains to be determined. Given the importance of phospholipid synthesis during S-phase of the cell cycle, the demonstration that FAS inhibitors induce ER stress in tumor cells also compliments a previous study that established that FAS inhibitors induce apoptosis during S-phase (42, 43). Collectively, the data presented herein fill a critical gap in our understanding of how endogenous fatty acid synthesis is required to maintain proper ER integrity and function.

We have demonstrated that inhibiting FAS activity in tumor cells induces an ER stress response. Based on these findings, we propose that one teleological explanation for high FAS levels in tumors is to provide support for a dynamic ER in rapidly proliferating cells. Furthermore, we hypothesize that the ER acts as a sensor of FAS activity and resulting phospholipid levels. In addition, we demonstrate that orlistat and C75 cooperate with the ER stressing agent thapsigargin to enhance cell death in vitro. While thapsigargin is highly toxic and not a likely candidate for tumor therapy, these data implies that tumor microenvironment-induced ER stress will not hinder the efficacy of FAS inhibitors (44). The data also suggest that

FAS inhibitors might be combined with PERK inhibitors to enhance tumor cell cytotoxicity. In summary, these data provide the first evidence that FAS inhibitors induce ER stress, which may explain some anti-tumor effects of FAS inhibitors, and they also establish an important mechanistic link between FAS and ER function in tumor cells.

References

1. Wakil SJ. Fatty acid synthase, a proficient multifunctional enzyme. Biochemistry 1989;28:4523-30.
2. Asturias FJ, Chadick JZ, Cheung IK, et al. Structure and molecular organization of mammalian fatty acid synthase. Nat Struct Mol Biol 2005;12:225-32.
3. Milgraum LZ, Witters LA, Pasternack GR, Kuhajda FP. Enzymes of the fatty acid synthesis pathway are highly expressed in in situ breast carcinoma. Clinical Cancer Research 1997;3:2115-20.
4. Pizer ES, Pflug BR, Bova GS, et al. Increased fatty acid synthase as a therapeutic target in androgen-independent prostate cancer progression. Prostate 2001;47:102-10.
5. Kuhajda FP. Fatty acid synthase and cancer: new application of an old pathway. Cancer Res 2006;66:5977-80.
6. Rossi S, Graner E, Febbo P, et al. Fatty acid synthase expression defines distinct molecular signatures in prostate cancer. Mol Cancer Res 2003;1:707-15.
7. Kuhajda FP. Fatty-acid synthase and human cancer: new perspectives on its role in tumor biology. Nutrition 2000;16:202-8.
8. Kuhajda FP, Jenner K, Wood FD, et al. Fatty acid synthesis: a potential selective target for antineoplastic therapy. Proceedings of the National Academy of Sciences of the United States of America 1994;91:6379-83.
9. Kuhajda FP, Pizer ES, Li JN, et al. Synthesis and antitumor activity of an inhibitor of fatty acid synthase. Proc Natl Acad Sci USA 2000;97:3450-54.
10. Alli PM, Pinn ML, Jaffee EM, McFadden JM, Kuhajda FP. Fatty acid synthase inhibitors are chemopreventive for mammary cancer in neu-N transgenic mice. Oncogene 2005;24:39-46.
11. Pizer ES, Jackisch C, Wood FD, et al. Inhibition of fatty acid synthesis induces programmed cell death in human breast cancer cells. Cancer Research 1996;56:2745-47.
12. Wang HQ, Altomare DA, Skele KL, et al. Positive feedback regulation between AKT activation and fatty acid synthase expression in ovarian carcinoma cells. Oncogene 2005;24:3574-82.
13. Kridel SJ, Axelrod F, Rozenkrantz N, Smith JW. Orlistat is a novel inhibitor of fatty acid synthase with antitumor activity. Cancer Res 2004;64:2070-5.
14. Menendez JA, Vellon L, Lupu R. Antitumoral actions of the anti-obesity drug orlistat (XenicalTM) in breast cancer cells: blockade of cell cycle progression, promotion of apoptotic cell death and PEA3-mediated transcriptional repression of Her2/neu (erbB-2) oncogene. Ann Oncol 2005;16:1253-67.
15. Knowles LM, Axelrod F, Browne CD, Smith JW. A fatty acid synthase blockade induces tumor cell-cycle arrest by down-regulating Skp2. J Biol Chem 2004;279:30540-5.
16. Hatzivassiliou G, Zhao F, Bauer DE, et al. ATP citrate lyase inhibition can suppress tumor cell growth. Cancer Cell 2005;8:311-21.
17. Brusselmans K, De Schrijver E, Verhoeven G, Swinnen JV. RNA interference-mediated silencing of the acetyl-CoA-carboxylase-alpha gene induces growth inhibition and apoptosis of prostate cancer cells. Cancer Res 2005;65:6719-25.
18. Chajes V, Cambot M, Moreau K, Lenoir GM, Joulin V. Acetyl-CoA Carboxylase {alpha} Is Essential to Breast Cancer Cell Survival. Cancer Res 2006;66:5287-94.

19. Sriburi R, Jackowski S, Mori K, Brewer JW. XBP1: a link between the unfolded protein response, lipid biosynthesis, and biogenesis of the endoplasmic reticulum. J Cell Biol 2004;167:35-41.
20. van der Sanden MHM, Meems H, Houweling M, Helms JB, Vaandrager AB. Induction of CCAAT/Enhancer-binding Protein (C/EBP)-homologous Protein/Growth Arrest and DNA Damage-inducible Protein 153 Expression during Inhibition of Phosphatidylcholine Synthesis Is Mediated via Activation of a C/EBP-activating Transcription Factor-responsive Element. J Biol Chem 2004;279:52007-15.
21. Cox JS, Chapman RE, Walter P. The unfolded protein response coordinates the production of endoplasmic reticulum protein and endoplasmic reticulum membrane. Mol Biol Cell 1997;8:1805-14.
22. Swinnen JV, Van Veldhoven PP, Timmermans L, et al. Fatty acid synthase drives the synthesis of phospholipids partitioning into detergent-resistant membrane microdomains. Biochem Biophys Res Commun 2003;302:898-903.
23. Brewer JW, Diehl JA. PERK mediates cell-cycle exit during the mammalian unfolded protein response. PNAS 2000;97:12625-30.
24. Feng B, Yao PM, Li Y, et al. The endoplasmic reticulum is the site of cholesterol-induced cytotoxicity in macrophages. Nat Cell Biol 2003;5:781-92.
25. Harding HP, Zhang Y, Khersonsky S, et al. Bioactive small molecules reveal antagonism between the integrated stress response and sterol-regulated gene expression. Cell Metab 2005;2:361-71.
26. Kaufman RJ. Regulation of mRNA translation by protein folding in the endoplasmic reticulum. Trends Biochem Sci 2004;29:152-8.
27. Bi M, Naczki C, Koritzinsky M, et al. ER stress-regulated translation increases tolerance to extreme hypoxia and promotes tumor growth. Embo J 2005;24:3470-81.
28. Harding HP, Zhang Y, Bertolotti A, Zeng H, Ron D. Perk is essential for translational regulation and cell survival during the unfolded protein response. Mol Cell 2000;5:897-904.
29. Calfon M, Zeng H, Urano F, et al. IRE1 couples endoplasmic reticulum load to secretory capacity by processing the XBP-1 mRNA. Nature 2002;415:92-6.
30. Zinszner H, Kuroda M, Wang X, et al. CHOP is implicated in programmed cell death in response to impaired function of the endoplasmic reticulum. Genes Dev 1998;12:982-95.
31. Luo S, Baumeister P, Yang S, Abcouwer SF, Lee AS. Induction of Grp78/BiP by translational block: activation of the Grp78 promoter by ATF4 through and upstream ATF/CRE site independent of the endoplasmic reticulum stress elements. J Biol Chem 2003;278:37375-85.
32. Gray MD, Mann M, Nitiss JL, Hendershot LM. Activation of the UPR is necessary and sufficient for reducing topoisomerase II {alpha} protein levels and decreasing sensitivity to topoisomerase targeted drugs. Mol Pharmacol 2005.
33. Ma Y, Hendershot LM. Delineation of a negative feedback regulatory loop that controls protein translation during endoplasmic reticulum stress. J Biol Chem 2003;278:34864-73.
34. Heiligtag SJ, Bredehorst R, David KA. Key role of mitochondria in cerulenin-mediated apoptosis. Cell Death Differ 2002;9:1017-25.
35. Tessitore A, del PMM, Sano R, et al. GM1-ganglioside-mediated activation of the unfolded protein response causes neuronal death in a neurodegenerative gangliosidosis. Mol Cell 2004;15:753-66.

36. Ramanadham S, Hsu FF, Zhang S, et al. Apoptosis of insulin-secreting cells induced by endoplasmic reticulum stress is amplified by overexpression of group VIA calcium-independent phospholipase A2 (iPLA2 beta) and suppressed by inhibition of iPLA2 beta. Biochemistry 2004;43:918-30.
37. Reimold AM, Etkin A, Clauss I, et al. An essential role in liver development for transcription factor XBP-1. Genes Dev 2000;14:152-7.
38. Lee A-H, Iwakoshi NN, Glimcher LH. XBP-1 Regulates a Subset of Endoplasmic Reticulum Resident Chaperone Genes in the Unfolded Protein Response. Mol Cell Biol 2003;23:7448-59.
39. Xu C, Bailly-Maitre B, Reed JC. Endoplasmic reticulum stress: cell life and death decisions. J Clin Invest 2005;115:2656-64.
40. Harding HP, Zhang Y, Zeng H, et al. An Integrated Stress Response Regulates Amino Acid Metabolism and Resistance to Oxidative Stress. Molecular Cell 2003;11:619-33.
41. Bandyopadhyay S, Zhan R, Wang Y, et al. Mechanism of Apoptosis Induced by the Inhibition of Fatty Acid Synthase in Breast Cancer Cells. Cancer Res 2006;66:5934-40.
42. Zhou W, Simpson PJ, McFadden JM, et al. Fatty Acid Synthase Inhibition Triggers Apoptosis during S Phase in Human Cancer Cells. Cancer Res 2003;63:7330-37.
43. Jackowski S, Wang J, Baburina I. Activity of the phosphatidylcholine biosynthetic pathway modulates the distribution of fatty acids into glycerolipids in proliferating cells. Biochimica et Biophysica Acta (BBA) - Molecular and Cell Biology of Lipids 2000;1483:301-15.
44. Fels DR, Koumenis C. The PERK/eIF2alpha/ATF4 Module of the UPR in Hypoxia Resistance and Tumor Growth. Cancer Biol Ther 2006;5:723-8.

Figure Legends

Figure 1. Fatty acid synthase inhibitors induce phosphorylation of eIF2α in tumor cells. A, PC-3 cells were treated with the indicated concentrations of orlistat (left) or cerulenin (middle) for 16 hours, or C75 (10 μg/ml) for 8-24 hours (right). Samples were resolved by SDS-PAGE, transferred to PVDF and the membrane was probed with antibodies specific for phospho-eIF2α, total eIF2α and β-tubulin. B, PC-3 cells were treated for two hours with C75 (10 μg/ml), orlistat (25 μM, 50μM), or cerulenin (5 μg/ml, 10 μg/ml), then incubated with ^{14}C-acetate (1 μCi) for two hours. Cells were collected, washed and lipids were extracted and quantified relative to vehicle-treated control (left). PC-3 cells were treated with orlistat (50 μM) for the indicated times or thapsigargin (Tgn, 1 μM) for one hour and then pulsed with 10 μCi ^{35}S-methionine for thirty minutes. Protein aliquots were then resolved by SDS-PAGE and new protein synthesis was quantified by scanning on a Typhoon 9210. Quantification is relative to vehicle treated control (right). C, PC-3 cells were transfected with siRNA against FAS or luciferase (Luc) for the indicated times and analyzed by immunoblot. D, FS-4 normal foreskin fibroblasts were treated with orlistat (25 μM) for 24 hours or thapsigargin (1 μM) for one hour side by side with PC3 cells and prepared for immunoblot analysis.

Figure 2. PERK phosphorylates eIF2α is response to, and protects cells against, orlistat treatment. A, Wild-type (WT) and *PERK*$^{-/-}$ MEFs transformed with *Ki-Ras*^{V12} were treated with orlistat (12.5 μM) for the indicated times. Samples were analyzed with antibodies specific for phospho-eIF2α and total eIF2α. B, Clonogenic survival assays were performed in WT and

PERK$^{-/-}$ MEFs, treated with vehicle, orlistat (25 μM) or Tgn (100 nM) for 16 hours, in triplicate. The surviving fraction was normalized relative to vehicle treated controls. C, HT-29 cells and HT-29/ΔC-PERK cells were treated with vehicle, orlistat (25 μM), C75 (9 μg/ml) or Tgn (10 nM) for 16 hours, in triplicate. Clonogenic survival was normalized relative to vehicle treated controls and statistical significance was determined by two-tailed Student's *t* tests.

Figure 3. FAS inhibitor treatment activates processing of XBP-1. A, PC-3 cells were treated with orlistat (50 μM) for the indicated times or Tgn (500 nM) for 8 hours. B, PC-3 cells were treated with the indicated concentrations of cerulenin for 16 hours or Tgn (500 nM) for 8 hours. C, HeLa cells were transfected with siRNA against FAS or luciferase (Luc) for the indicated times. D, PC-3 and FS- 4 cells were treated with orlistat (50 μM) for 16 hours or Tgn (1 μM) for one hour. Total RNA was collected and RT-PCR was performed as described in experimental procedures. XBP-1 is indicated by the 473 bp product and XBP-1(s) is indicated by the 447 bp fragment.

Figure 4. Inhibition of FAS activity induces mRNA expression of ER stress regulated genes. A, DU145 cells were treated with vehicle control, orlistat (50 μM, top), C75 (9 μg/ml, bottom), or Tgn (500 nM) for 16 hours. B, PC-3 cells were transfected with siRNA against FAS or luciferase (Luc) for 72 hours. C, PC-3 cells were treated with vehicle control or orlistat (25 μM) for 24 hours or Tgn (1μM) for one hour. Total RNA was collected with TRIzol and semi-quantitative RT-PCR was performed with oligonucleotides specific for CHOP (A and B), GRP78 and ATF4 (C) or β-actin (A-C).

Figure 5. Phosphorylation of eIF2α is an early event in cells treated with FAS inhibitors. A, PC-3 cells were treated with 50 μM orlistat for the indicated times and samples were collected for immunoblot analysis and probed with antibodies specific for phospho-eIF2α, cleaved PARP, cleaved caspase 3, and β-actin. B, PC-3 cells were treated with DMSO, cycloheximide (CHX, 1 μg/ml), orlistat (25 μM) or orlistat with CHX for 16 hours. Clonogenic survival was normalized relative to vehicle treated controls. C, PC-3 cells were treated with DMSO, cycloheximide (1μg/ml), orlistat (25μM), or the combination of orlistat and CHX for 16 hours. Samples were collected for immunoblot analysis and probed with antibodies specific for phospho-eIF2α, total eIF2α, and β-tubulin.

Figure 6. Pharmacological FAS inhibitors cooperate with thapsigargin. A, PC-3 cells were treated with DMSO, C75 (9 μg/ml), thapsigargin (25 nM) or the combination of each for 12 hours and clonogenic survival was normalized relative to vehicle treated controls (left). Times and doses of these various experiments were selected to achieve minimal cell kill from single agents, so that the effect of the combination would be most clear. PC-3 cells were treated with DMSO, C75 (9 μg/ml), thapsigargin (25 nM) or the combination of both for 20 hours and samples were subjected to immunoblot analysis (top right), or RNA was collected and semi-quantitative RT-PCR was performed using primers specific for GADD34 or β-actin (bottom right). B, HT-29 were treated with DMSO, orlistat (25 μM), thapsigargin (25 nM) or the combination of each for 12 hours (left). Cells were treated with DMSO, C75 (9 μg/ml), thapsigargin (25 nM) or the combination of each for 12 hours (right). Clonogenic survival was normalized relative to vehicle treated controls. C, Model demonstrating that in a proliferating tumor cell FAS contributes to ER function by driving phospholipid synthesis (left). When FAS is

inhibited (right), ER stress is induced which activates a series of downstream events that mediate adaptation and promote ER membrane biogenesis.

Little, J.L., et al. Figure 1

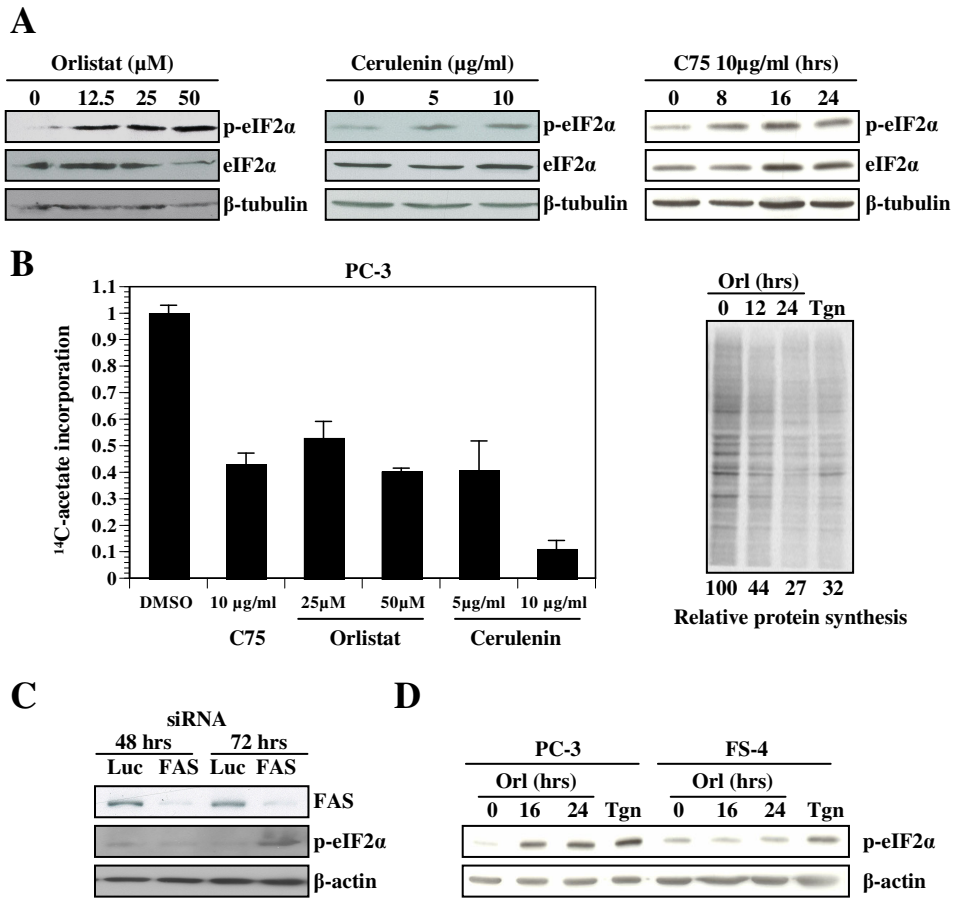

Little, J.L., et al. Figure 2

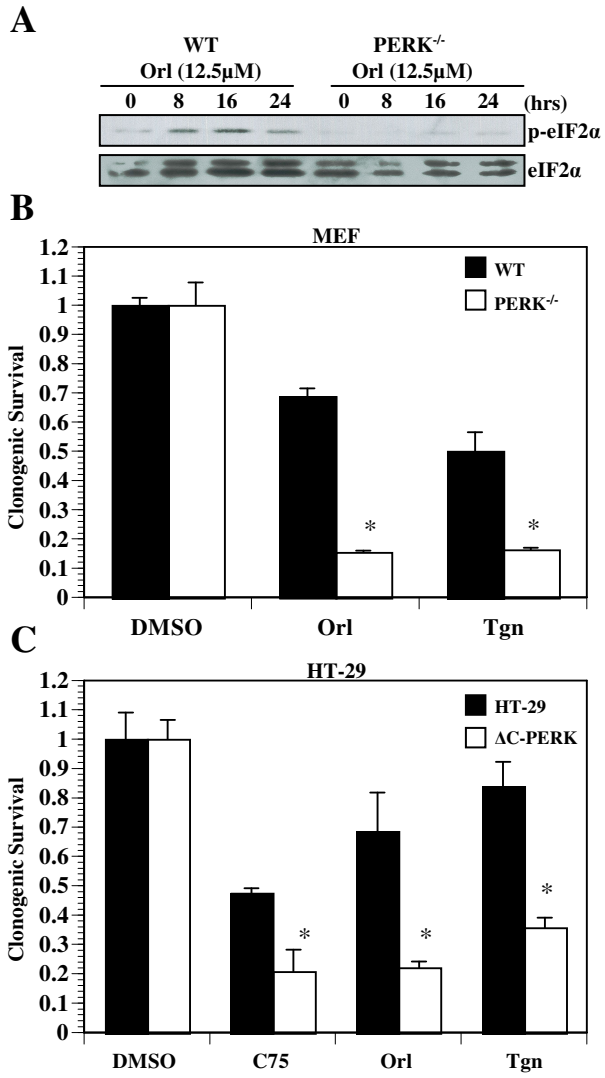

Little, J.L., et al. Figure 3

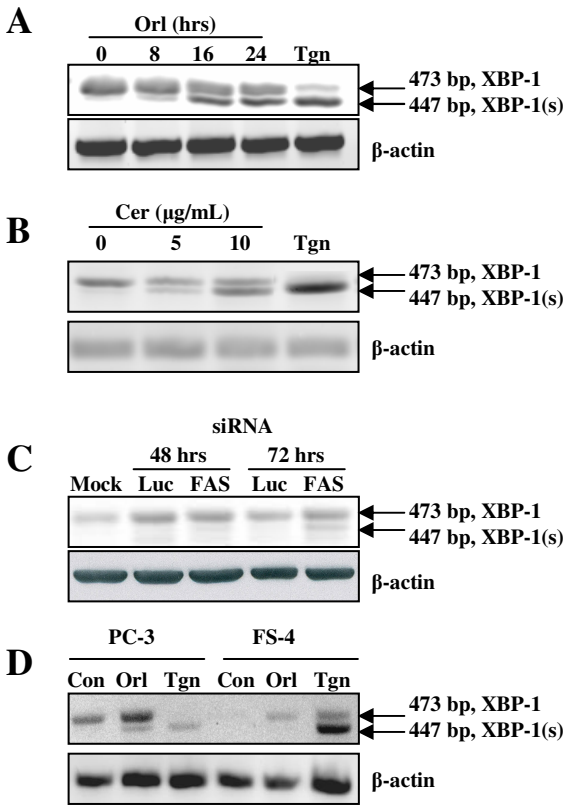

Little, J.L., et al. Figure 4

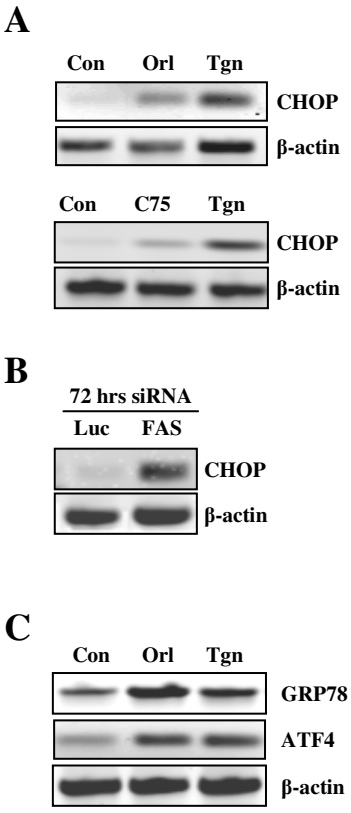

Little, J.L., et al. Figure 5

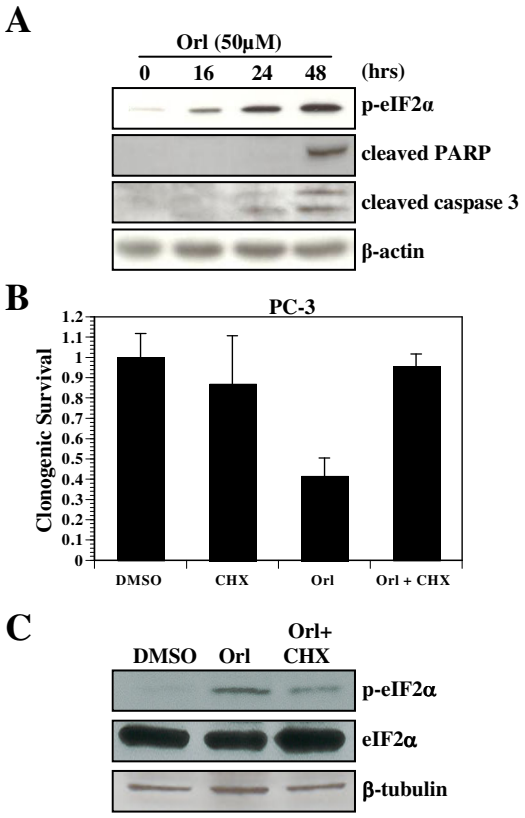

Little, J.L., et al. Figure 6

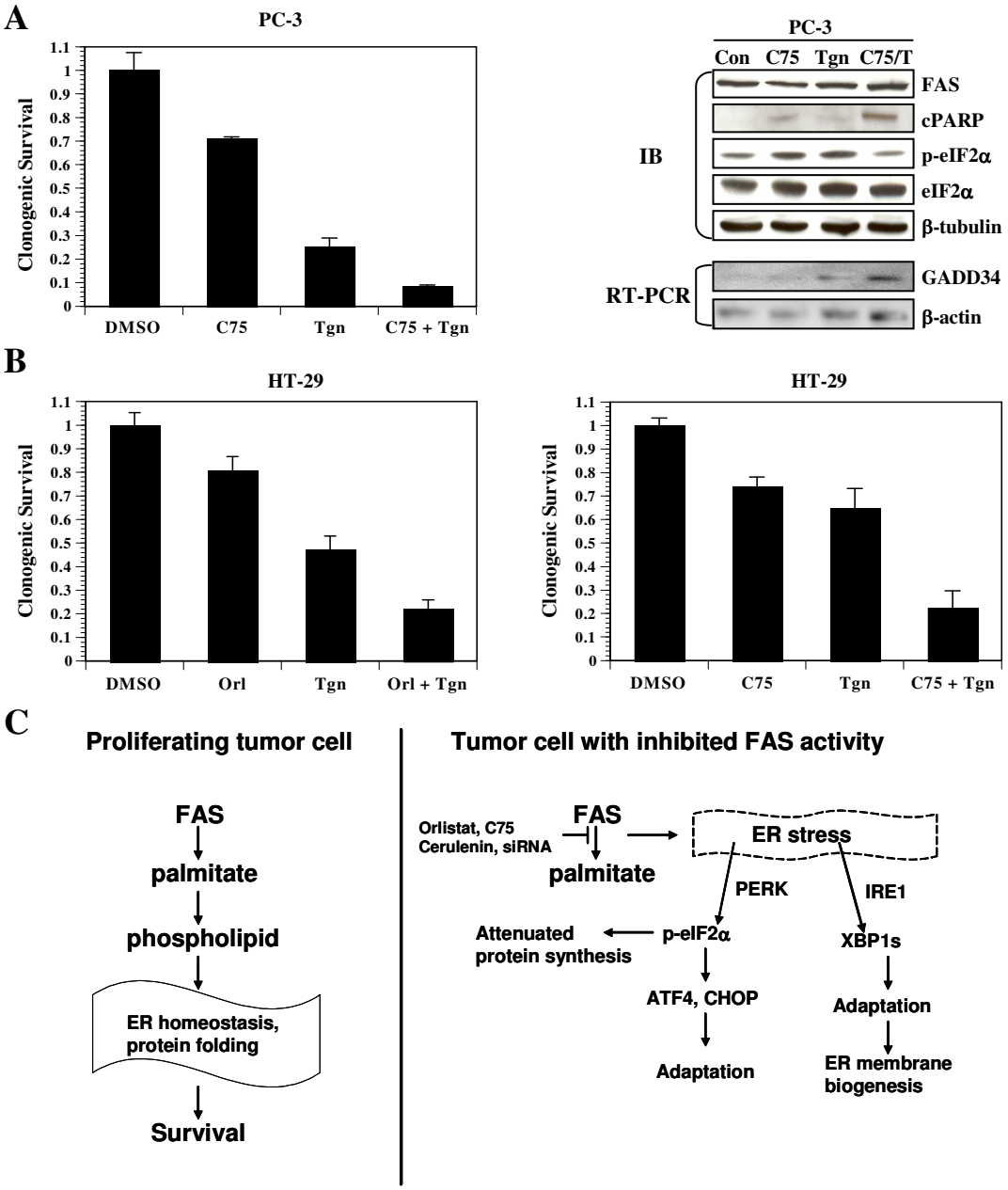

British Journal of Cancer (2006) 95, 869 – 878

www.bjcancer.com

Fatty acid synthase: a novel target for antiglioma therapy

W Zhao*[,1], S Kridel[2], A Thorburn[2], M Kooshki[1], J Little[2], S Hebbar[1] and M Robbins[1]

[1]Departments of Radiation Oncology and Neurosurgery, Brain Tumor Center of Excellence, Wake Forest University School of Medicine, Medical Center Boulevard, Winston-Salem, NC 27157, USA; [2]Department of Cancer Biology, Wake Forest University School of Medicine, Winston-Salem, NC 27157, USA

High levels of fatty acid synthase (FAS) expression have been observed in several cancers, including breast, prostate, colon and lung carcinoma, compared with their respective normal tissue. We present data that show high levels of FAS protein in human and rat glioma cell lines and human glioma tissue samples, as compared to normal rat astrocytes and normal human brain. Incubating glioma cells with the FAS inhibitor cerulenin decreased endogenous fatty acid synthesis by approximately 50%. Cell cycle analysis demonstrated a time- and dose-dependent increase in S-phase cell arrest following cerulenin treatment for 24 h. Further, treatment with cerulenin resulted in time- and dose-dependent decreases in glioma cell viability, as well as reduced clonogenic survival. Increased apoptotic cell death and PARP cleavage were observed in U251 and SNB-19 cells treated with cerulenin, which was independent of the death receptor pathway. Overexpressing Bcl-2 inhibited cerulenin-mediated cell death. In contrast, primary rat astrocytes appeared unaffected. Finally, RNAi-mediated knockdown of FAS leading to reduced FAS enzymatic activity was associated with decreased glioma cell viability. These findings suggest that FAS might be a novel target for antiglioma therapy.
British Journal of Cancer (2006) **95,** 869 – 878. doi:10.1038/sj.bjc.6603350 www.bjcancer.com
Published online 12 September 2006

Keywords: fatty acid synthase; glioma cells; cerulenin; cell cycle arrest; apoptosis; Bcl-2

In 2006, 18 820 individuals living in the US will be diagnosed with primary brain cancer (Jemal *et al*, 2006). The most common and most lethal primary brain tumour in adults is glioblastoma multiforme. Glioblastoma multiforme represents one of the most challenging of all cancers to treat successfully, characterised not only by aggressive proliferation and expansion but also by inexorable tumour invasion into distant brain tissue (Kew and Levin, 2003). Improvements in multimodality treatments including surgery, radiotherapy, and the recent addition of temozolomide have improved median survival, but this is still only approximately 14 months (Stupp *et al*, 2005) and long-term survival is dismal. The development of novel biological therapies for primary brain tumours remains an urgent need. Current cancer treatment is rapidly evolving in parallel with an understanding of tumour biology (Weiss, 2000; Karpati and Nalbantoglu, 2003). Genetic abnormalities and differential gene expression between normal and cancer cells can provide novel targets for anticancer therapy (Lang *et al*, 1999; Bansal and Engelhard, 2000; Grill *et al*, 2001).

Fatty acid synthase (FAS) is a 270 kDa cytosolic multifunctional polypeptide and is the primary enzyme required for catalysing the conversion of dietary carbohydrates to fatty acids (Wakil, 1989). Normal cells preferentially use circulating dietary fatty acids for the synthesis of new structural lipids. Thus, FAS expression is generally low to undetectable in normal human tissues, other than the liver and adipose tissue. In contrast, FAS is overexpressed in many human tumours, including carcinoma of the breast (Milgraum *et al*, 1997; Wang *et al*, 2001b), prostate (Epstein *et al*, 1995; Swinnen *et al*, 2002), colon (Rashid *et al*, 1997), ovary (Gansler *et al*, 1997), endometrium (Pizer *et al*, 1998b), mesothelium (Gabrielson *et al*, 2001), lung (Piyathilake *et al*, 2000), thyroid (Vlad *et al*, 1999), and stomach (Kusakabe *et al*, 2002). Abnormally active endogenous fatty acid metabolism appears to be important for cancer cell proliferation and survival (Ookhtens *et al*, 1984). Moreover, overexpression of FAS in breast, prostate, and thyroid cancers has been associated with more aggressive malignancies (Epstein *et al*, 1995; Gansler *et al*, 1997; Vlad *et al*, 1999; Swinnen *et al*, 2002). The preferential expression of FAS in cancer cells suggests that FAS could be a promising target for antitumour therapy (Kuhajda, 2006).

Inhibitors of FAS have been used to study the loss of FAS function in tumour cells. The first identified 'specific' inactivator of FAS, cerulenin, (2*R*, 3*S*)-2,3-epoxy-4-oxo-7,10-trans,trans-dodecadienamide, is a natural antibiotic product of the fungus *Cephalosporium ceruleans* (Omura, 1976). Cerulenin irreversibly inhibits FAS by binding covalently to the active site cysteine thiol in the β-ketoacyl-synthase domain (Funabashi *et al*, 1989). Cerulenin is selectively cytotoxic to a number of established human cancer cell lines, including breast (Gabrielson *et al*, 2001), colon (Pizer *et al*, 1998a), and prostate (Furuya *et al* 1997; Pizer *et al*, 2001). Kuhajda *et al* (2000) reported that cerulenin inhibited fatty acid synthesis in tumour cells in a dose-dependent manner; the cytotoxic effect of cerulenin to human breast tumour cells generally paralleled the level of endogenous fatty acid synthesis. Fatty acid synthase inhibition by cerulenin leads to apoptotic cell death in breast, prostate, and colon cancer cells (Furuya *et al*, 1997; Huang *et al*, 2000; Li *et al*, 2001). However, cerulenin's chemical instability renders it inappropriate as a systemic anticancer agent. C75, a potent derivative of cerulenin and a more stable form of FAS inhibitor, has been tested recently for its anti-breast tumour effects

*Correspondence: Dr W Zhao; E-mail: wzhao@wfubmc.edu
Revised 1 August 2006; accepted 8 August 2006; published online 12 September 2006

(Kuhajda *et al*, 2000; Pizer *et al*, 2000). *In vivo* and *in vitro* studies have confirmed the selective toxicity of C75 against tumour cells. C75-mediated inhibition of FAS increases malonyl-CoA levels and inhibits CPT-1 activity, preventing the oxidation of newly synthesised fatty acids. High levels of malonyl-CoA and CPT-1 inhibition might represent a mechanism, whereby FAS inhibition leads to tumour cell death (Pizer *et al*, 2000). C75 treatment of mesothelioma and prostate cancer xenografts in nude mice led to significant inhibition of tumour growth (Gabrielson *et al*, 2001; Pizer *et al*, 2001). Subcutaneous xenografts of MCF7 breast cancer cells in nude mice treated with C75 showed fatty acid synthesis inhibition, apoptosis, and inhibition of tumour growth to less than 12.5% of control volumes, without comparable toxicity in normal tissues (Pizer *et al*, 2000).

More recently, an activity-based proteomics strategy revealed *in vitro* and *in vivo* antitumour activity for Orlistat, an FDA-approved drug used for treating obesity. Orlistat is a novel inhibitor of the thioesterase domain of FAS that inhibited prostate cancer cell proliferation, induced apoptosis, and inhibited the growth of PC-3 human tumour xenografts implanted in nude mice (Kridel *et al*, 2004).

To date, there is little information regarding FAS expression in brain tumours. Slade *et al* (2003) reported that significantly larger amounts of FAS protein were detected in the neuroblastoma cell line SK-N-SH compared with that in the human fibroblast cell line Hs27. We hypothesised that FAS would be highly expressed in glioma cells and that inhibition of FAS would lead to glioma cell death. In this paper, we show that this hypothesis appears to be correct. For the first time, we show upregulation of FAS in glioma cells and human glioma tissue, dose-and time-dependent decreases in glioma cell viability, and clonogenic survival with FAS inhibition, as well as increased apoptotic cell death. These studies identify FAS as a potential target for glioma therapy.

Translational Therapeutics

MATERIALS AND METHODS

Cell culture

Human U373, U118, U87, and U138 as well as rat C6 glioma cell lines were obtained from the American Type Culture Collection (Rockville, MD, USA). The ethyl nitrosourea-induced rat 36B10 glioma cell line was obtained from Dr Vincent Traynelis, Division of Neurosurgery, Department of Surgery, University of Iowa (Spence & Coates, 1978) and routinely maintained in high glucose DMEM containing 5% bovine calf serum, 2 mM L-glutamine, 100 IU ml^{-1} penicillin, 100 μg ml^{-1} streptomycin, and 0.1 mM non-essential amino acids (all from GIBCO, Gaithersburg, MD, USA) at 37°C with 5% CO_2 in air. Cells were trypsinised and reseeded at a 1:5 dilution every 3 days. Human U251 and SNB-19 glioma cell lines were a kind gift of Dr Sue Hess (Department of Radiation Oncology, WFUSM) and were maintained in DMEM/F12 and F10 media supplemented with 10% foetal bovine serum (FBS), 2 mM L-glutamine, 100 IU ml^{-1} penicillin, and 100 μg ml^{-1} streptomycin. Primary rat astrocytes were isolated from 1- to 2-day-old Sprague–Dawley rat pups as described previously (Murphy, 1990). Cortices were removed from the rat pups; the meninges were stripped and homogenised. After incubation with trypsin for 15 min in a 37°C shaking water bath, the homogenate was centrifuged and the pellet was resuspended in a trypsin inhibitor/DNAse solution, triturated, and layered over a bovine serum albumin solution. The cell pellet was resuspended and maintained in MEM medium with 1% L-glutamine, 10% FBS, and 6 g l^{-1} glucose at 37°C in a humidified atmosphere of 5% CO_2 until ready to use.

Human glioma and normal brain tissue

Human brain tissue lysates were prepared by homogenisation in modified RIPA buffer (150 mM sodium chloride, 50 mM Tris-HCl (pH 7.4), 1 mM phenyl methyl sulphonyl fluoride, 1% Triton X-100, 1% sodium deoxycholic acid, 0.1% sodium dodecyl sulphate (SDS), 5 μg ml^{-1} aprotinin, and 5 μg ml^{-1} leupeptin). The tissue lysates were centrifuged for 10 min at 10 000 r.p.m. to remove debris and the supernatants were stored at −80°C until use.

Fatty acid synthesis

To test whether cerulenin inhibits FAS activity in glioma cells, lipid synthesis was determined using ^{14}C-labelled acetic acid methods as described previously (Rashid *et al*, 1997). Briefly, 5×10^5 SNB-19, U251, and C6 cells were plated into 24-well plates for 24 h (three replicates per group). After incubation with 5 μg ml^{-1} cerulenin for 2 h at 37°C, the cells were washed and were then incubated with ^{14}C-labelled acetate for 4 h. Total lipids were extracted and ^{14}C counts determined using liquid scintillation counting.

Western blot analysis

Western blot analysis was performed as described previously (Zhao *et al*, 2001). Cells were lysed using lysis buffer containing 50 mM Tris (pH 7.0), 1 mM EDTA, 150 mM NaCl, 1 mM PMSF, 1 μg ml^{-1} aprotinin, 1 μg ml^{-1} leupeptin, 1 mM Na_3VO_4, and 1 mM NaF, and stored in aliquots at −70°C until use. Ten micrograms of cell lysate was mixed with an equal volume of sample buffer containing 62.5 mM Tris/HCl (pH 6.8), 10% glycerol, 2% SDS, 5% β-mercaptoethanol, and 2–3 drops of saturated bromophenol solution, denatured by boiling, and separated in a 7.5% polyacrylamide mini-gel at a constant voltage of 120 V for 2 h. The proteins were transferred by electrophoresis at 100 V for 1 h to ECL nitrocellulose membrane (Amersham, Arlington Heights, IL, USA). The membranes were blocked for 1 h at room temperature in 5% (wt vol^{-1}) non-fat dry milk in TTBS containing 20 mM Tris-HCl (pH 7.0), 137 mM NaCl, and 0.05% (vol vol^{-1}) Tween-20. After washing in TTBS for 2 × 10 min, the membranes were then blocked with 5% non-fat milk and probed with either primary mouse anti-FAS (Pharmingen, San Diego, CA, USA), mouse anti-Bcl-2 (Santa Cruz, Santa Cruz, CA, USA), or rabbit anti-poly(ADP-ribose) polymerase (PARP) antibody (Athens Biotech, Athens, GA, USA). After washing three times in TBST for 10 min each, the blots were incubated with anti-mouse or anti-goat IgG horseradish peroxidase conjugate (1:10 000 dilution, Sigma, St Louis, MO, USA) for 1 h at room temperature. Antigen was detected using standard chemical luminescence methodology (ECL; Amersham Pharmacia Biotech, Piscataway, NJ, USA).

Cell viability assay

Cell viability was determined using a modified MTT assay (Griscelli *et al*, 2000). Briefly, 1000–5000 cells well^{-1} were plated in 24-well plates and incubated overnight. Cells were then treated with 0.5–10 μg ml^{-1} cerulenin for 24–144 h. At the end of the follow-up period, MTT in PBS was added and the cultures were incubated for 4 h at 37°C. The dark crystals formed were dissolved by adding to the wells an equal volume of SDS/dimethylformamide (DMF) extraction buffer (20% SDS and 50% N, N-DMF (pH 4.7), in PBS). Subsequently, plates were incubated overnight at 37°C. A 100 μl aliquot of the soluble fraction was transferred into 96-well microplates, and the absorbance at 570 nm was measured using an ELISA plate reader.

Clonogenic survival assay

Clonogenic survival assays were performed as described previously (Vartak *et al*, 1998). Two hundred and fifty to 2000 cells were plated in 60 mm dishes and incubated overnight. Cells were then treated with 0–10 μg ml^{-1} cerulenin and cultured until colonies had formed (10–14 days). Cells were then fixed for 10 min in a

solution containing 10% acetate and 10% methanol. The cells were then stained with 0.4% crystal violet for another 10 min. The crystal violet was removed and cells were washed with tap water until clear. Colonies containing $\geqslant 50$ cells were counted. For each experiment, four culture dishes were performed and experiments were carried out in triplicate. Surviving fraction was calculated from the number of colonies formed in the cerulenin-treated dishes compared with the number formed in the untreated control, where plating efficiency is defined as the percentage of cells plated that form colonies, and surviving fraction = number of colonies formed/(number of cells plated $\times$ plating efficiency).

Irradiation

Cells were irradiated with a range of single doses of 0–8 Gy of γ rays using a ^{137}Cs self-shielded irradiator at a dose rate of 4.0 Gy min^{-1}. All irradiations were performed at room temperature; control cells received sham irradiation. After irradiation, the culture plates were returned to the incubator and maintained at 37°C for 96 h. Cell viability was assessed using the MTT assay described above.

Flow cytometric analysis of cell cycle status

Flow cytometric evaluation of the cell cycle was performed using a modified protocol (Amant *et al*, 2003). Briefly, 5×10^5 cells were plated on 100 mm dishes in medium complemented with 10% FBS overnight. The culture medium was then replaced using serum-free medium for 24 h and the cells treated with 0–10 μg ml^{-1} cerulenin for 24 h. Cells were then trypsinised and collected into ice-cold PBS, and fixed with ice-cold 70% ethanol in PBS for at least 24 h at 4°C. Cells were then stained using 1 ml propidium iodide (PI) solution (20 mg l^{-1} PI and 20 mg l^{-1} RNase in PBS) for 3 h and read on a flow cytometer (Beckman-Coulter, Fullerton, CA, USA).

Fatty acid synthase shRNA constructs

The nucleotide targets of the FAS coding sequence were selected based on previously published experiments (De Schrijver *et al*, 2003) and computer-based target analysis using siRNA Target Finder (Ambion Inc., Austin, TX, USA). Two 19 base pair siRNA oligonucleotides were used in our study according to siRNA selective guidelines (Ambion Inc.). The first oligonucleotide was AACCCTGAGATCCCAGCGCTG, corresponding to the nucleotides 1212–1231 of human FAS; the second oligonucleotide was AAGCAGGCACACACGATGGAC, corresponding to the nucleotides 329–348. The two target sequences were aligned to the human genome in a BLAST search to eliminate those with significant homology to other genes. A scrambled nucleotide sequence was designed and used as the negative control. The loop sequences and overhangs were added to form the short hairpin constructs. Then, the short hairpin RNA (shRNA) encoding oligonucleotides were cloned into the *Bam*H1 and *Hin*dIII restriction sites downstream of the H1 promoter in pSilencer 3.0-H1 according to the manufacturers' instructions (Invitrogen, Grand Island, NY, USA).

Transient transfection

Transient transfections were performed using Lipofectamine according to the manufacturer's instructions (Invitrogen). Briefly, 5×10^6 cells were plated in a 60 mm dish supplied with 5 ml media for 24 h. Cells were then washed twice with serum- and antibiotic-free DMEM medium. Four micrograms of FAS RNAi plasmids/scrambled negative control plasmid and 20 μl Lipofectamine were premixed for 20 min and applied to cells in 4 ml serum- and antibiotic-free DMEM medium. After 4 h, the serum- and antibiotic-free DMEM medium was replaced with 5 ml of complete medium.

Stable transfection

U251 cells were grown on 60 mm dishes for 24 h and were then transfected with 2 μg of the endoplasmic reticulum (ER)-targeted GFP-Bcl-2 expression vector, wild-type (WT) GFP-Bcl-2 expression vector, or empty vector (gift of Dr Clark W Distelhorst, Case Western Reserve University Medical School and University Hospitals of Cleveland, Cleveland, OH, USA) using Lipofectamine plus reagent according to manufacturer's protocol (Life Technologies). The positive transfected cells were selected in the presence of the neomycin-analogue G418 (800μg ml^{-1}).

Dominant-negative FADD expression

Recombinant doxycycline (Dox)-regulated YFP and dominant-negative YFP-FADD-DN adenoviruses were made using the AdenoX Tet-off kit from Clontech (Palo Alto, CA, USA). Viruses were produced according to the manufacturer's instructions. Dominant-negative adenovirus FADD-DN or adenovirus YFP (empty vector) were co-infected into U251 and SNB-19 glioma cells with a Tet repressor virus. Once FAD-DN was expressed at high levels, as demonstrated by robust YFP fluorescence, cells were treated as required.

Statistical analysis

Statistical analysis was carried out using one-sample Student's *t*-test to compare differences between the treated cells and their appropriate controls. A *P*-value of <0.05 was considered significant.

RESULTS

Fatty acid synthase is overexpressed in human and rat glioma cell lines as well as in human glioma tissue samples

To determine if there is differential expression in glioma cells compared with normal brain cells, we measured FAS protein levels in six human glioma cell lines, U251, U373, U138, U118, U87, and SNB-19 and in two rat glioma cell lines, C6 and 36B10, as well as in primary rat astrocytes. Cells were cultured and lysed in 500 μl lysis buffer containing 50 mM Tris-HCl (pH 7.4), 150 mM NaCl, 1% NP-40, 0.25% Na-deoxycholate, and 1 mM of EDTA, PMSF, Na_3VO_4 and NaF, and proteinase inhibitors. Fatty acid synthase protein levels were analysed by Western blotting. As shown in Figure 1A, a low level of FAS protein was detected in normal primary astrocytes. In contrast, markedly elevated levels of FAS protein were observed in the entire human and rat glioma cell lines. Densitometric analysis revealed 4- to 20-fold increases in FAS expression in the glioma cell lines in comparison with that seen in primary rat astrocytes (Figure 1B). Elevated levels of FAS protein, ranging from 2- to 3.5-fold increases, were also observed in lysates of human glioma tissue samples compared with those obtained from normal human brain (Figure 1C and D).

Treating glioma cells with the FAS inhibitor cerulenin leads to inhibition of fatty acid synthesis

Cerulenin, a potent noncompetitive pharmacological inhibitor of FAS, binds covalently to the active site of the condensing enzyme region, inactivating a key enzyme step in fatty acid synthesis. To confirm the inhibitory effect of cerulenin on FAS in glioma cells, fatty acid synthesis activity was measured using the ^{14}C-labelled acetic acid method (Rashid *et al*, 1997). U251 and SNB-19 human glioma as well as C6 rat glioma cells were incubated with or without cerulenin for 2 h. After labelling with ^{14}C-actic acid, the total lipid was extracted and the amount of ^{14}C incorporated in the extracted total lipids was determined using liquid scintillation

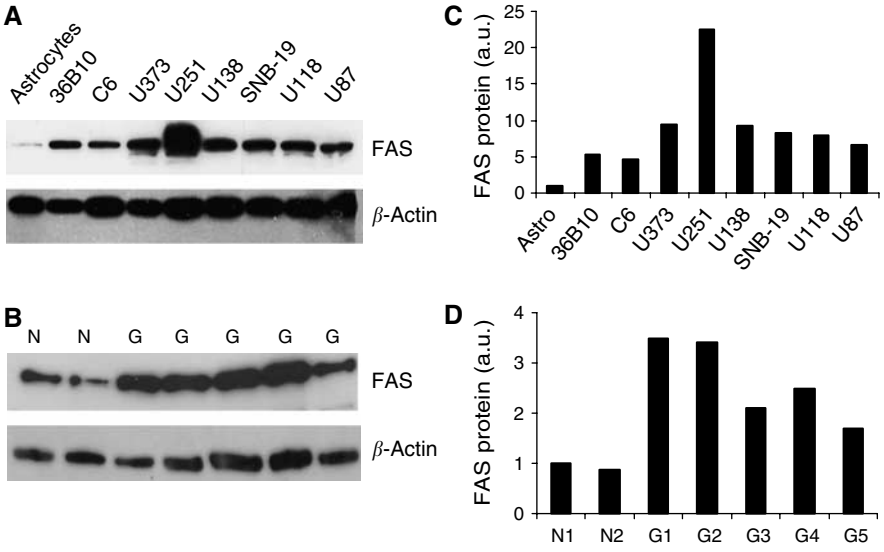

Figure 1 Fatty acid synthase is overexpressed in human and rat glioma cell lines and in human glioma tissue compared with primary rat astrocytes and normal human brain tissue, respectively. U138, U251, U373, SNB-19 human, and C6 rat glioma cells, as well as primary rat astrocytes were grown on 100 mm dishes until 90% confluent. The protein level of FAS was analysed by Western immunoblotting using a monoclonal mouse anti-FAS antibody; β-actin protein level was used as a loading control. (**A**) A representative Western Blot indicating the differential expression of FAS in rat and human glioma cell lies as well as primary rat astrocytes. (**C**) The mean densitometric values obtained from two independent experiments. (**B**) A Western blot of lysates obtained from normal human brain as well as several human glioma tissue samples. (**D**) The densitometric analysis of these blots.

counting. As shown in Figure 2, endogenous fatty acid synthesis in cerulenin-treated glioma cells decreased by approximately 50% in SNB-19, U251, and C6 cells compared with untreated controls. Fatty acid synthase activity was not detectable in primary rat astrocytes (data not shown).

Incubating glioma cells with cerulenin leads to selective time- and dose-dependent decreases in glioma cell viability and survival; normal astrocytes appear unaffected

To demonstrate whether cerulenin is selectively cytotoxic to glioma cells, we measured the effects of cerulenin on glioma cells and primary rat astrocytes using the MTT and/or clonogenic assay. U251, SNB-19, U87, U118 human, and C6 rat glioma cells were treated with 0–15 $\mu g\,ml^{-1}$ cerulenin for 24 and 96 h. We observed rounded up cells following incubation with higher doses (Figure 3A and B) in 24 h and cell death. As shown in Figure 3C, the mean IC_{50} values for U251 cells were 4.7 and 2.3 $\mu g\,ml^{-1}$ at 24 and 96 h, respectively. SNB-19 glioma cells showed a similar cytotoxic response to treatment with cerulenin; the mean IC_{50} values for SNB-19 cells were 5.3 and 2.6 $\mu g\,ml^{-1}$ at 24 and 96 h, respectively (Figure 4A). Moreover, treatment with cerulenin led to a significant reduction in glioma cell clonogenic survival; incubating SNB-19 cells with 3 $\mu g\,ml^{-1}$ cerulenin reduced clonogenic cell survival by 97% compared to non-treated controls (Figure 4B). We also compared the cytoxicity of cerulenin to C6 rat glioma cells and to normal primary rat astrocytes. After treatment with 10 $\mu g\,ml^{-1}$ of cerulenin for 24 h, glioma cell viability was reduced to less than 10%; the mean IC_{50} value was 6.5 $\mu g\,ml^{-1}$ (Figure 4C). In contrast, primary astrocytes appeared resistant to cerulenin treatment. Incubating astrocytes with 0.5–7.5 $\mu g\,ml^{-1}$ cerulenin for 24 h failed to affect cell viability (Figure 4D).

Cerulenin-induced cell death occurs via an apoptotic mechanism

Poly(ADP-ribose) polymerase, an enzyme catalysing the poly(ADP-ribosyl)ation of various nuclear proteins with NAD, has been

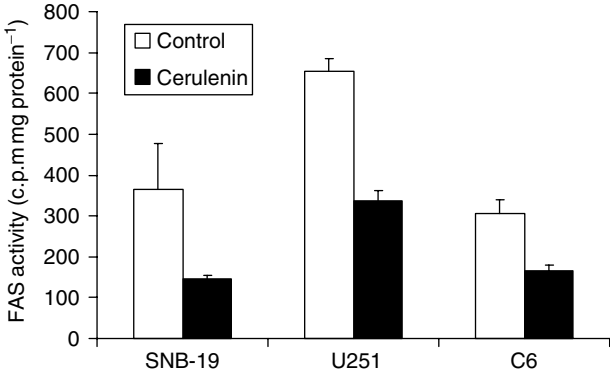

Figure 2 Treating glioma cells with the FAS inhibitor cerulenin leads to inhibition of fatty acid synthesis. U251 and SNB-19 human and C6 rat glioma cells were treated with 5 $\mu g\,ml^{-1}$ cerulenin for 2 h. Fatty acid synthesis activity was then measured using the ^{14}C-labelled acetate assay. Lipids were extracted and cerulenin-induced inhibition of labelled acetate incorporation into lipid was measured using liquid scintillation counting. Mean $\pm$ s.e.; $n = 3$; $^{*}P < 0.05$.

suggested to contribute to cell death by depleting the cell of NAD and ATP (Berger *et al*, 1983). Poly(ADP-ribose) polymerase cleavage is a well-established marker for apoptosis. To determine whether apoptosis is involved in cerulenin-induced cell cytotoxicity, we measured PARP cleavage as well as assessing morphological changes. As noted above, cell morphology was changed; cells appeared rounded up after incubation with cerulenin, resulting in cell death. To determine PARP cleavage, U251 and SNB-19 cells were treated with 0–10.0 $\mu g\,ml^{-1}$ cerulenin for 24 h and Western blot analysis was used to study the alterations in protein level of PARP in treated and non-treated glioma cells. Treatment with cerulenin led to a dose-dependent increase in cleaved PARP protein in both glioma cell lines (Figure 5).

Overexpressing Bcl-2 leads to inhibition of cerulenin-mediated cytotoxicity

Overexpression of the antiapoptotic protein Bcl-2 has been shown to inhibit cell death induced by several apoptotic signals and/or mediators (Wang *et al*, 2001a). To determine if overexpressing Bcl-2 would result in a similar inhibition of cerulenin-mediated apoptosis, U251 cells were stably transfected with either WT Bcl-2, ER-targeted Bcl-2, or empty vector. As shown in Figure 6A, transducing cells with Bcl-2 led to a marked increase in protein levels compared with the vector-transduced cells. U251 cells were then treated with 5 $\mu g\,ml^{-1}$ of cerulenin for 24 h, and cell viability assessed using the MTT assay. As noted previously, incubating U251 cells stably transfected with vector control alone with 5 $\mu g\,ml^{-1}$ cerulenin was associated with a reduction in cell viability to 55.5 + 3.4% of controls. Overexpressing ER/Bcl-2 and WT/Bcl-2 increased cell viability to 71.0 + 3.2 and 85.9 ± 2.8%, respectively ($P<0.05$; Figure 6).

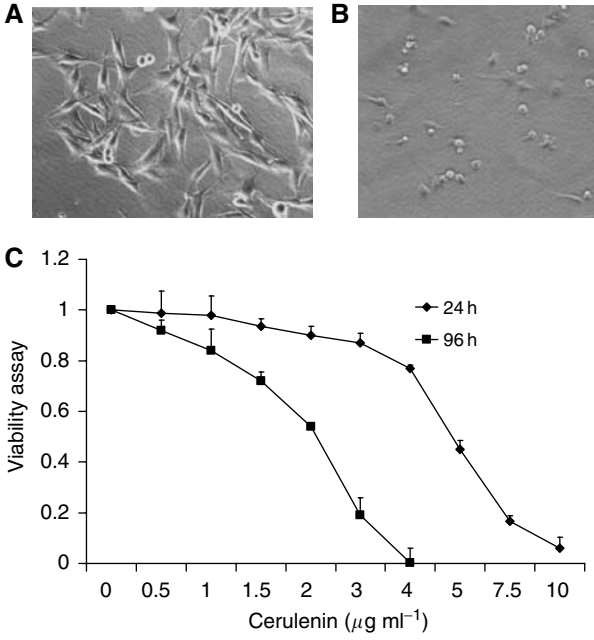

Figure 3 Cerulenin reduces U251 cell viability in a time- and dose-dependent manner. 5×10^4 or 5000 U251 human glioma cells were seeded into 24-well plates and treated with 0–10 $\mu g\,ml^{-1}$ cerulenin for 24 and 96 h, respectively. Cell viability was assessed using the MTT assy. (**A**) The morphological appearance of DMSO-treated control cells observed 24 h after treatment. (**B**) Incubating U251 glioma cells with cerulenin for 24 h resulted in the cells adopting a rounded up appearance. (**C**) Incubating U251 glioma cells with cerulenin cells led to a time- and dose-dependent reduction in cell viability. Mean ± s.e.; $n = 3$.

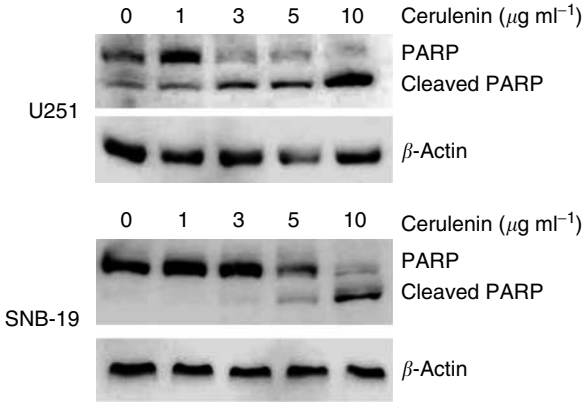

Figure 5 Cerulenin induces PARP cleavage in human glioma cells. U251 and SNB-19 cells were treated with 0–10 $\mu g\,ml^{-1}$ cerulenin for 24 h and then collected and lysed using lysis buffer. Poly(ADP-ribose) polymerase, cleaved PARP, and β-actin protein levels were analysed using Western blot. Representative Western blots show that cerulenin treatment was associated with dose-dependent increases in cleavage of PARP in both U251 (**A**) and SNB-19 (**B**) glioma cells. Data represent results of two independent experiments.

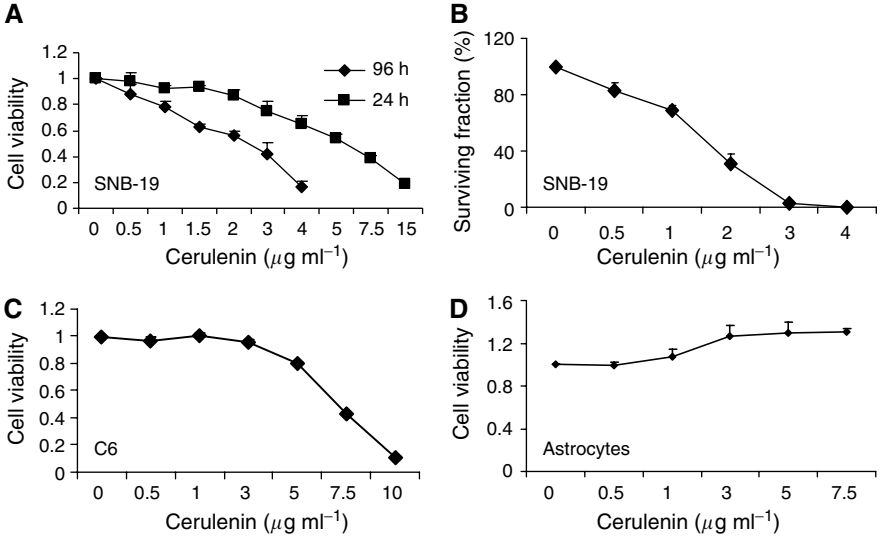

Figure 4 Cerulenin selectively reduces glioma cell viability and clonogenic survival; astrocytes are unaffected. 5×10^4 and 5000 SNB-19 human glioma cells were seeded into 24-well plates and treated with 0–10 $\mu g\,ml^{-1}$ cerulenin for 24 and 96 h, respectively. Cell viability was assessed using the MTT assay. To determine clonogenic survival, 500–2000 cells were seeded into 60 mm dishes and treated with 0–10 $\mu g\,ml^{-1}$ cerulenin for 10–15 days. Cells were fixed and stained with violet blue and colonies were counted using a colony counter. (**A**) Incubating SNB-19 cells with cerulenin led to a time- and dose-dependent reduction in cell viability. (**B**) A dose-dependent cerulenin-mediated reduction in clonogenic survival. (**C**) Incubating C6 rat glioma cells with cerulenin led to a time- and dose-dependent reduction in cell viability. In contrast, (**D**) shows that incubating primary rat astrocytes with 0.5–7.5 $\mu g\,ml^{-1}$ cerulenin for 24 h did not affect cell viability.

The death receptor FADD pathway is not involved in cerulenin-induced apoptosis

FADD-DN is a dominant-negative form of the FADD protein that blocks all known death receptor-induced apoptotic pathways. Activation of the death receptor pathway has been implicated in the mechanism of various chemotherapeutic agents that can work by upregulating death receptor levels or by raising autocrine production of death ligand. To test if such pathways contribute to cerulenin-induced apoptosis, U251 and SNB-19 cells were co-infected with adenoviruses expressing YFP or YFP-tagged FADD-DN. Fluorescence could be observed in infected cells (Figure 7B). After co-infection for 48 h, uninfected control cells, YFP-expressing cells, and YFP-FADD-DN-expressing cells were treated with 0–10 $\mu g\,ml^{-1}$ cerulenin for 24 h and the MTT assay was performed to measure cell viability. As shown in Figure 7C and D, no significant differences in cell viability were found in the various groups, indicating that the death receptor pathway is not associated with FAS inhibition-induced cell apoptosis.

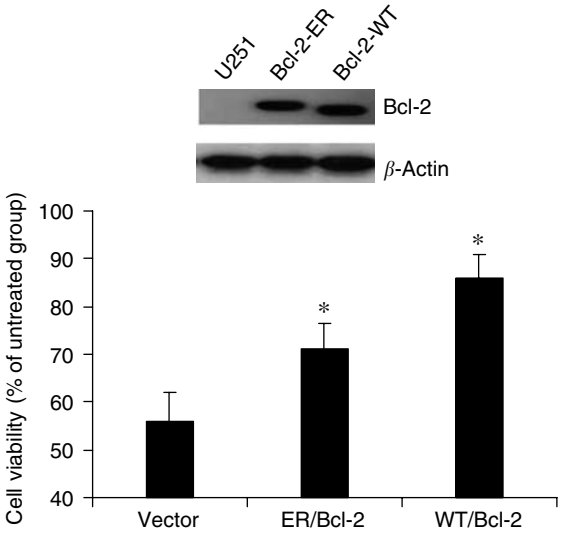

Figure 6 Bcl-2 overexpression protects U251 cells from cerulenin-induced cytotoxicity. U251 cells stably transfected with empty vector, ER-targeted vector, or WT Bcl-2 vector showed a marked increase in levels of Bcl-2 immunoreactive protein (**A**). Cells were treated with 5$\mu g\,ml^{-1}$ cerulenin for 24 h. Cell viability was then assessed using the MTT assay (**B**). Mean ± s.e.; $n = 4$, $P < 0.05$.

Treating human glioma cells with cerulenin leads to an S-phase cell cycle block

We hypothesised that the cerulenin-induced cell growth inhibition and death might involve cell cycle arrest. To test our hypothesis, we performed flow cytometry analysis. U251 and SNB-19 human glioma cells were treated with DMSO, 1 or 3 $\mu g\,ml^{-1}$ cerulenin for 24 h. The cells were then collected and stained with PI for flow cytometry analysis. Representative cell cycle profiles are shown in Figure 8. After treatment with cerulenin for 24 h, the number of U251 cells in S phase increased markedly to 58% of the total cell population compared with controls (23%). A similar increase in the % of cells in S phase was seen 24 h after treatment of SNB-19 cells with cerulenin (Figure 8). These results suggest that cerulenin-mediated FAS inhibition induced an S-phase block in glioma cells.

Pretreating glioma cells with cerulenin does not alter radiosensitivity

Cell radiosensitivity is cell cycle dependent; cells present in the S phase are relatively radioresistant as compared with cells in other phases of the cell cycle (Pawlik and Keyomarsi, 2004). As treating glioma cells with cerulenin induced an S-phase block, we hypothesised that irradiating glioma cells in the presence of cerulenin would lead to either no effect or increased radioresistance. As shown in Figure 9A, there was no difference in viability between glioma cells treated with 0.5–4.0 $\mu g\,ml^{-1}$ of cerulenin 2 h before irradiation with a single dose of 5 Gy of ^{137}Cs γ rays when compared with glioma cells treated with radiation alone. Increasing the time the cells were treated with cerulenin to 8 h before irradiation similarly failed to alter glioma cell radiosensitivity. Irradiating cerulenin-treated cells with single doses of

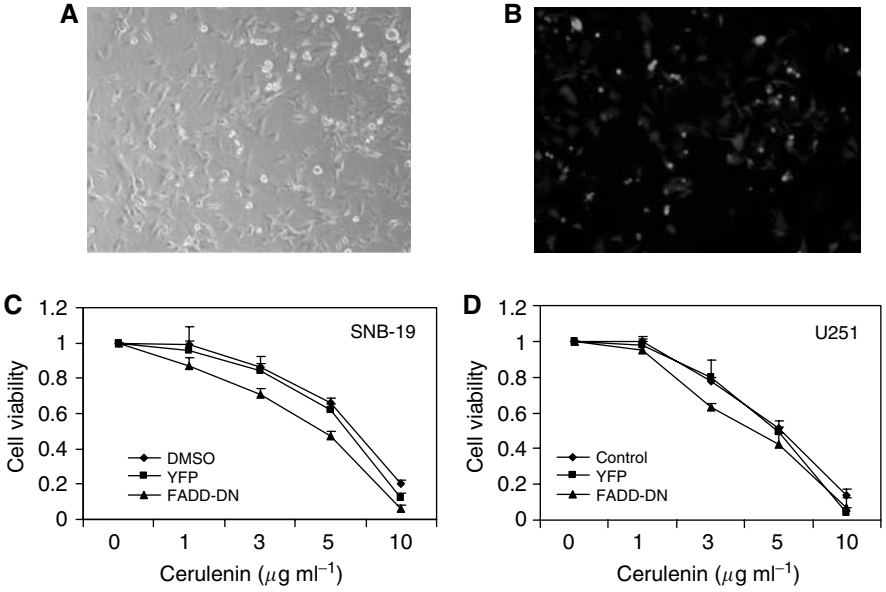

Figure 7 The death receptor FADD pathway is not involved in cerulenin-induced apoptosis. U251 and SNB-19 human glioma cells were co-infected with adenoviruses expressing YFP or TFP-tagged FADD-DN. (**A**) U251 cells treated with DMSO, (**B**) U251 cells co-infected with YFP-FADD-DN. Cells were then treated with 0–10 $\mu g\,ml^{-1}$ cerulenin for 24 h and cell viability was then assessed using the MTT assay. Co-infection with YFP or YFP-FADD-DN failed to inhibit the cerulenin-mediated glioma cell cytotoxicity.

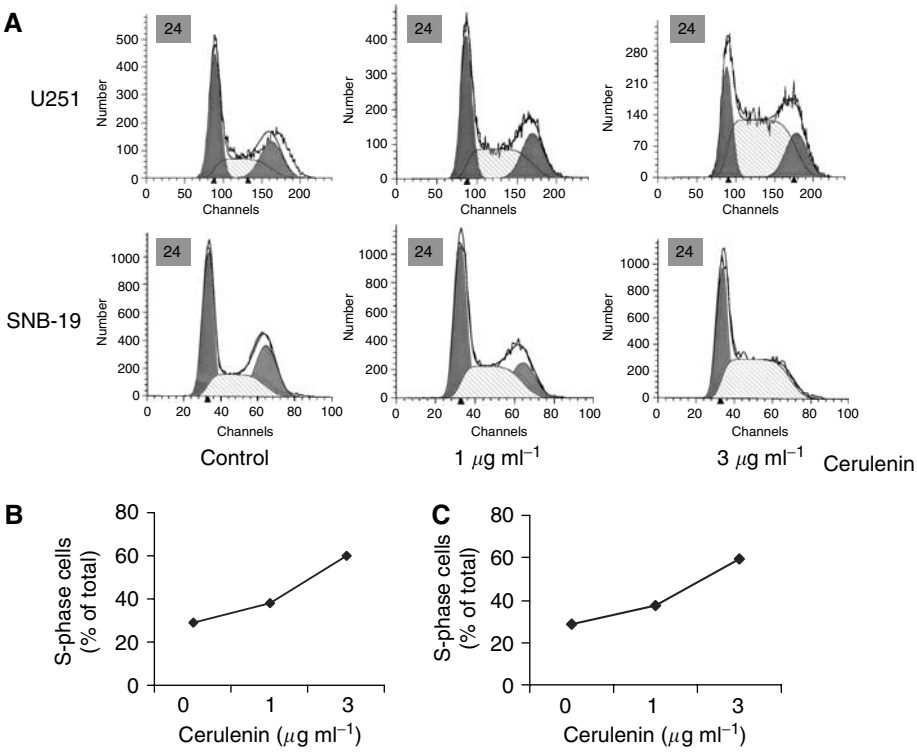

Figure 8 Treating human glioma cells with cerulenin leads to a dose-dependent accumulation of cells in S phase. U251 and SNB-19 human glioma cells were treated with DMSO, 1 μg ml^{-1} cerulenin, or 3 μg ml^{-1} cerulenin for 24 h. The cells were then harvested, fixed, stained with PI, and analysed by flow cytometry. (**A**) A representative flow cytometry experiment; (**B**) and (**C**) the mean data obtained from the results of two independent experiments. These data indicate that incubating U251 and SNB-19 cells with cerulenin led to a dose-dependent increase in S-phase cell accumulation.

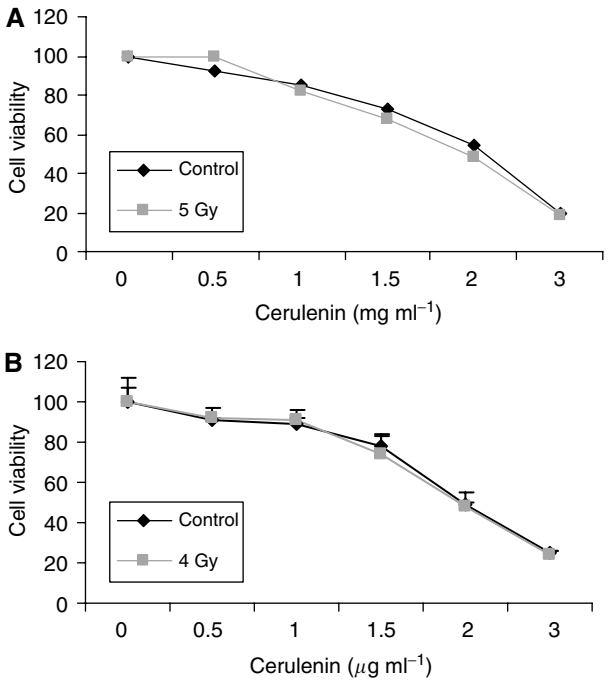

Figure 9 Treating human glioma cells with cerulenin fails to alter their radiosensitivity. SNB-19 human glioma cells were treated with 0.5–4.0 μg ml^{-1} cerulenin for 2 h, control cells received DMSO. The cells then received either γ irradiation (single dose of 4 or 5 Gy γ rays [■]) using a ^{137}Cs irradiator or sham irradiation (◆), incubated for 96 h, and then viability was assessed using the MTT assay.

2, 4, or 8 Gy had no affect on glioma cell radiosensitivity. Figure 9B shows data for glioma cells treated with cerulenin 8 h before a single dose of 4 Gy; a similar response was seen after doses of 2 and 8 Gy (data not shown).

Fatty acid synthase shRNA transfection leads to downregulation of FAS expression and enzymatic activity that is associated with decreased glioma cell viability

To confirm that the effects of cerulenin were due to inhibition of FAS, we used RNAi to knock down FAS protein levels. To identify effective RNAi against FAS expression, we tested two different plasmid-based hairpin constructs of FAS RNAi; a scrambled sequence was used as the negative control. The shRNAs encoding oligonucleotides are shown in Figure 10B. They were cloned into the *Bam*H1 and *Hin*dIII restriction sites downstream of the H1 promoter in pSilencer 3.0-H1 (Figure 10A). U251 and SNB-19 cells were seeded into 60 mm dishes for 24 h and transfected with 2 and 4 μg FAS shRNA DNA for a further 72 h. Cells were then lysed and FAS protein expression analysed using Western blot analysis. As shown in Figure 10C, scrambled shRNA (control) had no effect on FAS expression. In contrast, FAS shRNA1 and FAS shRNA2 reduced significantly FAS protein levels. Moreover, this reduction in FAS protein was associated with a significant ($P<0.05$) reduction in FAS enzymatic activity (Figure 10D). To test the effects of RNAi-mediated FAS silencing on glioma cell growth, SNB-19 cells were transiently transfected with a range of concentrations of plasmid DNA of scrambled shRNA and FAS shRNA for 72 h. Cytotoxicity was determined using the MTT assay. As shown in Figure 10E, cell viability was dose-dependently reduced in glioma cells transfected with FAS RNAi. These data confirm the effect of cerulenin as being FAS-specific.

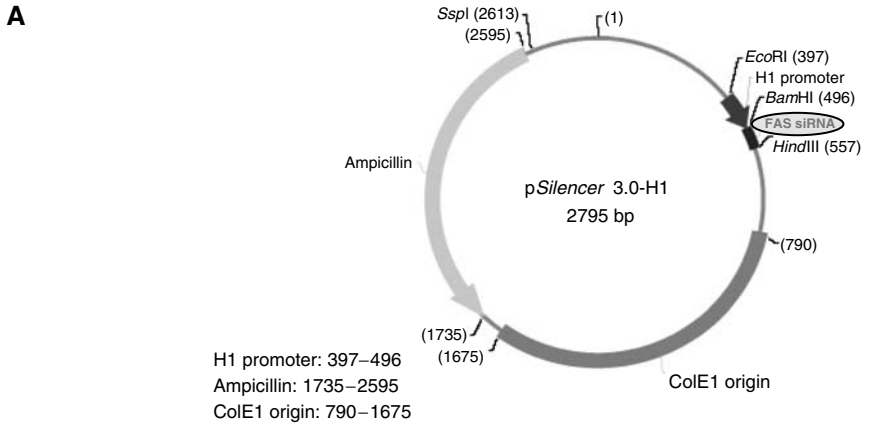

B

FAS RNAi-1:

5′-GATCCC*GCAGGCACACACGATGGAC*TTCAAGAGA*GTCCATCGTGTGTGCCTGC*TTTTTTGGAAA-3′
3′-GG*CGTCCGTGTGTGCTACCTGAA*GTTCTCT*CAGGTAGCACACACGGACG*AAAAAACCTTTTCGA-5′

FAS RNAi-2:

5′-GATCCCG*CCCTGAGATCCCAGCGCTG*TTCAAGAGA*CAGCGCTGGGATCTCAGGG*TTTTTTGGAAA-3′
3′-GGC*GGGACTCTAGGGTCGCGAC*AAGTTCTCT*GTCGCGACCCTAGAGTCCC*AAAAAACCTTTTCGA-5′

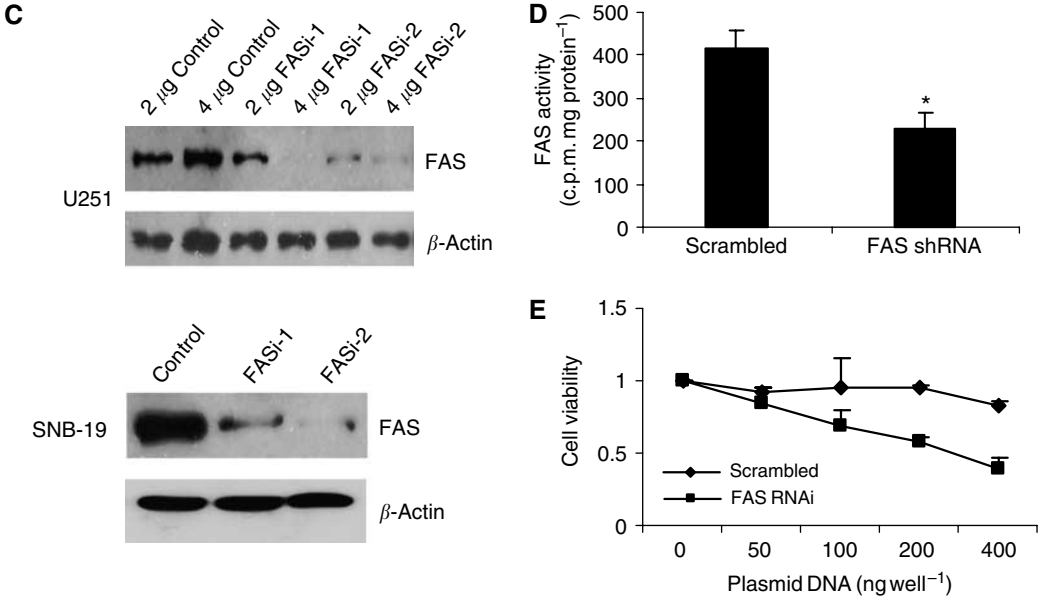

Figure 10 Fatty acid synthase shRNA transfection downregulates FAS expression and inhibits glioma cell growth. Sense and antisense oligonucleotides encoding the shRNAs (**B**) were cloned into the *Bam*H1 and *Hin*dIII restriction sites downstream of the H1 promoter in pSilencer 3.0H-1 (**A**). U251 and SNB-19 cells were seeded into 60 mm dishes for 24 h and transfected with 2 and 4 μg FAS shRNA DNA for a further 72 h. Cells were then lysed and FAS protein expression analysed using Western blot analysis. As shown in (**C**), FAS shRNA1 and FAS shRNA2 reduced markedly FAS protein levels; FAS enzymatic activity was also significantly reduced (**D**). Control cells transfected with a scrambled shRNA showed no change in FAS expression. As shown in (**E**), cell viability was significantly reduced in U251 glioma cells transfected with FAS RNAi.

DISCUSSION

Our data reveal, for the first time, that the levels of FAS expression observed in a variety of rat and human glioma cell lines and several human glioma tissue samples are higher compared to their normal cell counterpart, the astrocyte, as well as normal human brain tissue, respectively. Mammalian FAS is a multifunctional enzyme complex that catalyses the synthesis of palmitate from acetyl-CoA and malonyl-CoA with NADPH as a provider of reducing equivalents (Kuhajda, 2006). Humans take up large amount of proteins and lipids through their daily diet. Therefore, the levels of FAS in most tissues are low. In human tissue, FAS is distributed in cells involved in lipid metabolism and in hormone-sensitive cells, such as adipocytes, hepatocytes, sebaceous glands, and type II alveolar cells (Weiss *et al*, 1986). High FAS activity was observed in foetal brain tissue and gradually declined following aging (Salles *et al*, 2002). FAS mRNA level in 20-day-old rat brain was about 20% compared with that measured in 5-day-old brain (Garbay *et al*, 1997; Muse *et al*, 2001). In the adult rat brain, immunohistochemistical analysis for FAS revealed positive staining cells in cortical neurons of the frontooccipital lobes; only weak staining was observed in astrocytes (Kusakabe *et al*, 2000).

Glioma cell FAS expression has not been reported previously. We found a marked differential expression of FAS in glioma and normal astrocytes. A similar upregulation of FAS expression was noted in lysates of human glioma samples compared with lysates of

normal human brain tissue. Administration of the FAS inhibitor cerulenin led to significant time- and dose-dependent decreases in glioma cell viability and survival. Low doses of cerulenin caused cell cycle arrest, whereas higher doses led to cytotoxicity. In contrast, normal astrocytes were unaffected. These findings suggest that FAS might be a novel target for antiglioma therapy.

The mechanism(s) underlying malignant cell cytotoxicity following FAS inhibition has been studied in several cancer cell lines. FAS inhibition can cause accumulation of malonyl-CoA, which leads to inhibition of carnitine palmitoyltransferase-1 and, indirectly, the fatty acid oxidation pathway (Thupari *et al*, 2001). Rapid accumulation of malonyl-CoA was observed after FAS inhibition (Kuhajda *et al*, 2000). Blocking the accumulation of malonyl-CoA using 5-(tetradecyloxy)-2-furoic acid, an inhibitor of acetyl-CoA carboxylase, reduced significantly cerulenin- and C75-induced cytotoxicity and inhibition of breast tumour growth. Apoptosis appeared to play a major role in this cell death. In our experiments, we demonstrated clearly that PARP cleavage, an apoptotic marker, was induced in cerulenin-treated U251 and SNB-19 cells; this was associated with significant cytotoxicity. Heiligtag *et al* (2002) reported that cerulenin is an effective inducer of apoptosis in WT or mutant p53 neuroblastoma, melanoma, and colon carcinoma cell lines; normal human cells were resistant to cerulenin-induced apoptosis. Further, apoptosis was mediated both by overexpression of proapoptotic Bax, in a p53-independent manner, and by a rapid release of mitochondrial cytochrome *c*, leading to activation of caspase 3 and 9. Data presented in the current studies confirm a P53-independent apoptotic response in glioma cells following FAS inhibition; similar glioma cell cytotoxicity was observed in either P53 WT (U87 and U118) or in P53 mutant glioma cell lines (U251, SNB-19, U138, and C6).

Bcl-2, a protooncogene that enhances cell survival by inhibiting apoptosis (Vaux *et al*, 1988), is localised in the ER, the outer mitochondrial membrane, and the nuclear envelope (Akao *et al*, 1994). Stable expression of Bcl-2 or Bcl-2 targeted to the ER has been shown to inhibit apoptosis (Wang *et al*, 2001a). Similarly, we observed that stable expression of Bcl-2-targeted to the ER or WT Bcl-2 expressed not only in the ER but also in the mitochondria and nuclei, reduced cerulenin-mediated glioma cell death. These data provide additional support for the hypothesis that cerulenin-mediated toxicity is due, in part, to an increase in apoptotic cell death. To investigate further the apoptotic response, the role of the death receptor pathway in cerulenin-mediated apoptosis was evaluated by infecting glioma cells with a FADD-DN adenovirus. In agreement with the previously suggested mechanism involving cytochrome *c* release (Heiligtag *et al*, 2002) FADD-DN, which inhibits all the known death receptor pathways, had no effect on cerulenin-induced glioma cell death.

Cerulenin- and C75-mediated alterations in cell cycle progression have been observed in a variety of cancer cell lines. Although FAS inhibition can lead to a block in the cell cycle before G_1 (Kuhajda *et al*, 2000), there are data that support an S-phase arrest in breast cancer cells (Zhou *et al*, 2003) and in colon carcinoma cells (Pizer *et al*, 2001). In the current study, we demonstrated a marked, dose-dependent S-phase block at 24 h after treatment. The mechanism(s) of FAS inhibition-induced cell cycle arrest is still not clear. *De novo* fatty acid synthesis by tumour cells accounted for more than 93% of total lipid fatty acids in an experimental tumour model, indicating that endogenous fatty acid synthesis could be a significant source of fatty acids for tumour cell growth and survival (Ookhtens *et al*, 1984). Most of the fatty acids produced by tumour cells are incorporated into membrane phospholipids, and phospholipid synthesis is inhibited when fatty acid synthesis is inhibited (Pizer *et al*, 1996; Jackowski *et al*, 2000). Phospholipid biosynthesis is greatest during the G_1 and S phases, with doubling of the membrane mass occurring during S phase in preparation for cell division (Jackowski, 1994). Thus, cells in S phase should be most sensitive to changes in phospholipid metabolism. In contrast, cells in S phase are relatively radioresistant; the expected outcome would be either no effect or increased radioresistance. Indeed, as predicted, combining cerulenin treatment with ionising radiation did not alter glioma cell radioresistance.

We used selective gene silencing by siRNA (Zamore *et al*, 2000) to confirm the role of FAS inhibition in glioma cell cytotoxicity. RNAi-induced knockdown of FAS that led to a significant reduction in FAS enzymatic activity resulted in a dose-dependent reduction in glioma cell viability, confirming similar gene silencing approaches with RNAi described in human LNCaP prostate cancer cells (De Schrijver *et al*, 2003).

In conclusion, our studies demonstrate that (1) human and rat glioma cell lines express high levels of FAS compared with normal brain astrocytes; high levels of FAS were also seen in human glioma tissue compared with normal human brain, (2) FAS inhibition is selectively cytotoxic to glioma cells; normal astrocytes are unaffected; and (3) both cytotoxic and cytostatic effects contribute to the cerulenin-mediated effects in glioma cells. These findings support the hypothesis that FAS might be a novel target for antiglioma therapy.

ACKNOWLEDGEMENTS

This work was supported in part by NIH/NCI grant CA82722 (MER).

REFERENCES

Akao Y, Otsuki Y, Kataoka S, Ito Y, Tsujimoto Y (1994) Multiple subcellular localization of bcl-2: detection in nuclear outermembrane, endoplasmic reticulum membrane, and mitochondrial membranes. *Cancer Res* **54:** 2468 – 2471

Amant F, Lottering ML, Joubert A, Thaver V, Vergote I, Lindeque BG (2003) 2-methoxyestradiol strongly inhibits human uterine sarcomatous cell growth. *Gynecol Oncol* **91:** 299 – 308

Bansal K, Engelhard HH (2000) Gene therapy for brain tumors. *Curr Oncol* **2:** 463 – 472

Berger NA, Sims JL, Catino DM, Berger SJ (1983) In *ADP-ribosylation, DNA Repair and Cancer*. Miwa M, Hayaishi O, Shall S, Smulson M, Sugimura T (eds) pp. 219 – 226. Japan Scientific Society Press: Tokyo

De Schrijver E, Brusselmans K, Heyns W, Verhoeven G, Swinnen JV (2003) RNA interference-mediated silencing of the fatty acid synthase gene attenuates growth and induces morphological changes and apoptosis of LNCaP prostate cancer cells. *Cancer Res* **63:** 3799 – 3804

Epstein JI, Carmichael M, Partin AW (1995) OA-519 (fatty acid synthase) as an independent predictor of pathologic state in adenocarcinoma of the prostate. *Urology* **45:** 81 – 86

Funabashi H, Kawaguchi A, Tomoda H, Omura S, Okuda S, Iwasaki S (1989) Binding site of cerulenin in fatty acid synthetase. *J Biochem* **105:** 751 – 755

Furuya Y, Akimoto S, Yasada K, Ito H (1997) Apoptosis of androgen-independent prostate cell line induced by inhibition of fatty acid synthesis. *Anticancer Res* **17:** 4589 – 4593

Gabrielson EW, Pinn ML, Testa JR, Kuhajda FP (2001) Increased fatty acid synthase is a therapeutic target in mesothelioma. *Clin Cancer Res* **7:** 153 – 157

Gansler TS, Hardman III W, Hunt DA, Schaffel S, Hennigar RA (1997) Increased expression of fatty acid synthase (OA-519) in ovarian neoplasms predicts shorter survival. *Hum Pathol* **28:** 686 – 692

Garbay B, Bauxis-Lagrave S, Boiron-Sargueil F, Elson G, Cassagne C (1997) Acetyl-CoA carboxylase gene expression in the developing mouse brain.

Comparison with other genes involved in lipid biosynthesis. *Dev Brain Res* **98:** 197 – 203
Grill J, Van Beusechem VW, Van Der Valk P, Dirven CM, Lephart A, Pherai DS, Haisma HJ, Pinedo HM, Curiel DT, Gerritsen WR (2001) Combined targeting of adenoviruses to integrins and epidermal growth factor receptors increases gene transfer into primary glioma cells and spheroids. *Clin Cancer Res* **7:** 641 – 650
Griscelli F, Li H, Cheong C, Opolon P, Bennaceur-Griscelli A, Vassal G, Soria J, Soria, C, Lu H, Perricaudet M, Yeh P (2000) Combined effects of radiotherapy and angiostatin gene therapy in glioma tumor model. *Proc Natl Acad Sci USA* **97:** 6698 – 6703
Heiligtag SJ, Bredehorst R, David KA (2002) Key role of mitochondria in cerulenin-mediated apoptosis. *Cell Death Differ* **9:** 1017 – 1025
Huang PL, Zhu SN, Lu SL, Dai ZS, Jin YL (2000) Inhibitor of fatty acid synthase induced apoptosis in human colonic cancer cells. *World J Gastroenterol* **6:** 295 – 297
Jackowski S (1994) Coordination of membrane phospholipid synthesis with the cell cycle. *J Biol Chem* **269:** 3858 – 3867
Jackowski S, Wang J, Baburina I (2000) Activity of the phosphatidylcholine biosynthetic pathway modulates the distribution of fatty acids into glycerolipids in proliferating cells. *Biochim Biophys Acta* **1483:** 301 – 315
Jemal A, Siegel R, Ward E, Murray T, Xu J, Smigal C, Thun MJ (2006) Cancer statistics, 2006. *CA Cancer J Clin* **56:** 106 – 130
Karpati G, Nalbantoglu J (2003) The principles of molecular therapies for glioblastoma. *Int Rev Neurobiol* **55:** 151 – 163
Kew Y, Levin VA (2003) Advances in gene therapy and immunotherapy for brain tumors. *Curr Opin Neurol* **16:** 665 – 670
Kridel SJ, Axelrod F, Rosenkrantz N, Smith JW (2004) Orlistat is a novel inhibitor of fatty acid synthase with antitumor activity. *Cancer Res* **64:** 2070 – 2075
Kuhajda FP (2006) Fatty acid synthase and cancer: new application of an old pathway. *Cancer Res* **66:** 5977 – 5980
Kuhajda FP, Pizer ES, Li JN, Mani NS, Frehywot GL, Townsend CA (2000) Synthesis and antitumor activity of an inhibitor of fatty acid synthase. *Proc Natl Acad Sci USA* **97:** 3450 – 3454
Kusakabe T, Maeda M, Hoshi N, Sugino T, Watanabe K, Fukuda T, Suzuki T (2000) Fatty acid synthase is expressed mainly in adult hormone-sensitive cells or cells with high lipid metabolism and in proliferating fetal cells. *J Histochem Cytochem* **48:** 613 – 622
Kusakabe T, Nashimoto A, Honma K, Suzuki T (2002) Fatty acid synthase is highly expressed in carcinoma, adenoma and in regenerative epithelium and intestinal metaplasia of the stomach. *Histopathology* **40:** 71 – 79
Lang FF, Yung WK, Sawaya R, Tofilon PJ (1999) Adenovirus-mediated p53 gene therapy for human gliomas. *Neurosurgery* **45:** 1093 – 1104
Li J-N, Gorospe M, Chrest FJ, Kumaravel TS, Evans MK, Han WF, Pizer ES (2001) Pharmacological inhibition of fatty acid synthase activity produces both cytostatic and cytotoxic effects modulated by p53. *Cancer Res* **61:** 1493 – 1499
Milgraum LZ, Witters LA, Pasternack GR, Kuhajda FP (1997) Enzymes of the fatty acid synthesis pathway are highly expressed in *in situ* breast carcinoma. *Clin Cancer Res* **3:** 2115 – 2120
Murphy S (1990) Generation of astrocyte cultures from normal and neoplastic central nervous system. In *Methods in Neuroscience* Conn PM (ed.) pp. 33 – 47. New York: Academic Press
Muse ED, Jurevics A, Toews AD, Matsushima GK, Morell P (2001) Parameters related to lipid metabolism as markers of myelination in mouse brain. *J Neurochem* **76:** 77 – 86
Omura S (1976) The antibiotic cerulenin, a novel tool for biochemistry as an inhibitor of fatty acid synthesis. *Bact Rev* **40:** 681 – 697
Ookhtens M, Kannan R, Lyon I, Baker, N (1984) Liver and adipose tissue contributions to newly formed fatty acids in an ascites tumor. *Am J Physiol* **247:** R146 – R153
Pawlik TM, Keyomarsi K (2004) Role of cell cycle in mediating sensitivity to radiotherapy. *Int J Radiat Oncol Biol Phys* **59:** 928 – 942
Piyathilake CJ, Frost AR, Manne U, Bell WC, Weiss H, Heimburger DC, Grizzle WE (2000) The expression of fatty acid synthase (FASE) is an early event in the development and progression of squamous cell carcinoma of the lung. *Hum Pathol* **131:** 1068 – 1073
Pizer ES, Chrest FJ, DiGiuseppe JA (1998a) Pharmacological inhibitors of mammalian fatty acid synthase suppress DNA replication and induce apoptosis in tumor cell lines. *Cancer Res* **58:** 4611 – 4615
Pizer ES, Lax S, Kuhajda FP, Pasternak GR, Kurman RJ (1998b) Fatty acid synthase expression in endometrial carcinoma: correlation with cell proliferation and hormone receptors. *Cancer* **83:** 528 – 537
Pizer ES, Pflug BR, Bova GS, Han WF, Udan MS, Nelson JB (2001) Increased fatty acid synthase as a therapeutic target in androgen independent prostate cancer progression. *Prostate* **47:** 102 – 110
Pizer ES, Thupari J, Han WF, Pinn ML, Chrest FJ, Frehywot GL, Townsend CA, Kuhajda FP (2000) Malonyl-coenzyme-A is a potential mediator of cytotoxicity induced by fatty acid synthase inhibition in human breast cancer cells and xenografts. *Cancer Res* **60:** 213 – 218
Pizer ES, Wood FD, Pasternack GR, Kuhajda FP (1996) Fatty acid synthase (FAS): a target for cytotoxic antimetabolites in HL60 promyelocytic leukemia cells. *Cancer Res* **56:** 745 – 751
Rashid A, Pizer ES, Mog, M, Witters LA, Shy M, Jiang H, Cassagne C, Garbay B (1997) Elevated expression of fatty acid synthase and fatty acid synthetic activity in colorectal neoplasia. *Am J Pathol* **150:** 201 – 208
Salles J, Sargueil F, Knoll-Gellida A, Witters LA, Shy M, Jaing H, Cassagne C, Garbay B (2002) Fatty acid synthase expression during peripheral nervous system myelination. *Mol Brain Res* **101:** 52 – 59
Slade RF, Hunt DA, Pochet MM, Venema VJ, Hennigar RA (2003) Characterization and inhibition of fatty acid synthase in pediatric tumor cell lines. *Anticancer Res* **23:** 1235 – 1243
Spence AM, Coates PW (1978) Scanning electron microscopy of cloned astrocytic cell lines derived from ethyl nitrosourea-induced rat gliomas. *Virchows Archiv [B] Cell Pathol* **28:** 77 – 85
Stupp R, Mason WP, van den Bent MJ, Weller M, Fisher B, Taphoorn MJB, Belanger K, Brandes AA, Marosi C, Bogdahn U, Curschmann J, Janzer RC, Ludwin SK, Gorlia T, Allgeier A, Lacombe D, Cairncross JG, Eisenhauer E (2005) Radiotherapy plus concomitant and adjuvant temozolomide for glioblastoma. *N Engl J Med* **352:** 987 – 996
Swinnen JV, Roskams T, Joniau S, Van Poppel H, Oyen R, Baert L, Heyns W, Verhoeven G (2002) Overexpression of fatty acid synthase is an early and common event in the development of prostate cancer. *Int J Cancer* **98:** 19 – 22
Thupari JN, Pinn ML, Kuhajda FP (2001) Fatty acid synthase inhibition in human breast cancer cells leads to malonyl-CoA-induced inhibition of fatty acid oxidation and cytotoxicity. *Biochem Biophys Res Commun* **285:** 217 – 223
Vartak S, McCaw R, Davis CS, Robbins ME, Spector AA (1998) γ-Linolenic acid (GLA) is cytotoxic to 36B10 malignant rat astrocytoma cells but not to normal rat astrocytes. *Br J Cancer* **77:** 1613 – 1620
Vaux DL, Cory S, Adams JM (1988) Bcl-2 gene promotes haemopoietic cell survival and cooperates with c-myc to immortalize pre-B cells. *Nature* **335:** 440 – 442
Vlad LD, Axiotis C, Merino MJ, Green W (1999) Fatty acid synthase is highly expressed in aggressive thyroid tumors. *Mod Pathol* **12:** 70A
Wakil SJ (1989) Fatty acid synthase, a proficient multifunctional enzyme. *Biochemistry* **28:** 4523 – 4530
Wang NS, Unkila MT, Reineks EZ, Distelhorst CW (2001a) Transient expression of wild-type or mitochondrially targeted Bcl-2 induces apoptosis, whereas transient expression of endoplasmic reticulum-targeted Bcl-2 is protective against Bax-induced cell death. *J Biol Chem* **276:** 44117 – 44128
Wang Y, Kuhajda FP, Li JN, Pizer ES, Han WF, Sokoll LJ, Chan DW (2001b) Fatty acid synthase (FAS) expression in human breast cancer cell culture supernatants and in breast cancer patients. *Cancer Lett* **167:** 99 – 104
Weiss WA (2000) Genetics of brain tumor. *Curr Opin Pediat* **12:** 543 – 548
Weiss L, Hoffmann GE, Schreiber R, Andres H, Fuchs E, Korber E, Kohl HJ (1986) Fatty-acid biosynthesis in man, a pathway of minor importance. Purification, optimal assay conditions, and organ distribution of fatty-acid synthase. *Biol Chem Hoppe Seyler* **367:** 905 – 912
Zamore PD, Tuschl T, Sharp PA, Bartel, DP (2000) RNAi: double-stranded RNA directs the ATP-dependent cleavage of mRNA at 21 to 23 nucleotide intervals. *Cell* **101:** 25 – 33
Zhao W, Spitz DR, Oberley LW, Robbins MEC (2001) Redox modulation of the pro-fibrogenic mediator plasminogen activator inhibitor-1. *Cancer Res* **61:** 5537 – 5543
Zhou W, Simpson PJ, McFadden JM, Townsend CA, Medghalchi SM, Vadlamudi A, Pinn ML, Ronnett GV, Kuhjada FP (2003) Fatty acid synthase inhibition triggers apoptosis during S phase in human cancer cells. *Cancer Res* **63:** 7330 – 7337